

Evaluating enteric neuronal remodeling in individuals with combined upper and lower disorders of gut-brain interaction

Master's Degree Project in Biomedicine

Second Cycle 30 credits

Autumn semester 2025

Student: Ragaa Helal

Supervisor: Karolina Sjöberg Jabbar

Examiner: Homa Tajsharghi

Abstract

Overlap of irritable bowel syndrome (IBS) with gastroduodenal disorders of gut–brain interaction (DGBI) is common and associated with more severe symptoms, but the underlying causes of these severe symptoms are unknown. Here, neuropeptide signalling, neuronal plasticity, and compartment-specific nerve architecture in the colonic mucosa were examined in this phenotype. Colonic samples from healthy controls (HC, n=8) and IBS patients with or without gastroduodenal DGBI overlap (n=16 for each group) were examined for vasoactive intestinal polypeptide (VIP) and growth-associated protein-43 (GAP43) mRNA and protein expression. VIP and GAP43 were quantified by immunohistochemistry in the crypt, lamina propria, mucosa, and muscularis mucosa. These data were integrated with rectal barostat measurements of visceral sensitivity and with self-rating of anxiety, depression, and abdominal pain, using validated questionnaires. Non-parametric correlations and comparative statistics were used to analyse differences between groups, transcription–protein coupling, and associations with symptoms. IBS patients with DGBI overlap had higher VIP and GAP43 mRNA, but not protein, expression. For each protein, expression intensity correlated closely between mucosal layers in IBS participants but not in GAP43 in HC, whereas correlations with mRNA levels and symptoms were compartment-specific. Distinct, compartment-specific correlations between markers were observed in IBS with vs. without overlapping gastroduodenal DGBI. Lamina propria and mucosal GAP43 expression correlated inversely with abdominal pain in participants with IBS, which was largely driven by individuals with overlapping DGBI. Neuronal remodelling is differentially associated with abdominal pain and spatial neuronal distribution in the colonic mucosa in people with IBS with vs. without concomitant gastroduodenal DGBI.

Keywords: Disorders of gut-brain interaction, visceral hypersensitivity, enteric neuronal remodeling, abdominal pain, colonic mucosal innervation, Growth-associated protein 43.

Popular scientific summary

Irritable bowel syndrome (IBS) is mostly thought of as a disorder of gut motility, stress, inflammation, or sensitivity. However, new research shows that in a large subgroup of patients -those who also have chronic stomach and upper-gut symptoms- the problem may lie much deeper: in how the nerves inside the gut wall physically rearrange themselves. The gut contains its own huge and complex nervous system, often referred to as the “second brain”. It runs and branches throughout the gut wall layers, from the lining that meets food to the muscle layers that cause contractions. In healthy people, this system is well organized so that signals can flow smoothly between layers, and nerve growth is carefully controlled. This allows the gut to perceive what is happening inside it without causing pain.

In this study, two key nerve-related molecules were studied in colon biopsies. One called VIP, acts like a regulatory signal that helps in gut wall functions related to digestion and absorption. The other, called GAP43, signals nerves that are developing or wanting to connect. These markers show nerve number, location, and reconnecting activity. In healthy people, VIP is uniformly linked across all gut layers, forming a steady network from the gut surface to muscle. However, uncoupled GAP43 shows that nerve growth occurs quietly and locally, only where needed. None of these nerve activity cause pain or discomfort in healthy people. This means that under normal circumstances, the enteric nervous system does not generate symptoms.

In IBS patients with chronic upper-gut diseases, including functional dyspepsia or gastroduodenal illnesses, this design fails. Their gut wall tends to stimulate VIP and GAP43 genes for growth. Total nerve protein doesn't increase but rather gets reorganized improperly. Absence of nerve growth in the gut's protective surface layer, along with redirection of growth into the deeper muscular layers, which control gut wall contraction and sensitivity, was observed to cause pain in this study. This means that typical actions may cause discomfort due to the overstimulation of the nerves.

The picture is different for IBS patients without upper-gut involvement. They tend to show compensation in the form of encouraged nerve sprouting towards the surface, which may prevent pain. These findings challenge our views of persistent gut pain. They show that some patients may have misdirected nerve organization rather than more sensitive nerves. Understanding this could allow new treatments to restore the gut's nerve architecture, enabling its “second brain” to wire itself appropriately.

Contents

Abstract.....	
Popular scientific summary	
1 Introduction.....	1
2 Materials and Methods.....	3
2.1 Study population.....	3
2.1.1 Inclusion and exclusion criteria.....	3
2.2 Symptom Questionnaires.....	4
2.3 Assessment of visceral sensitivity.....	4
2.4 Sigmoidoscopy and biopsy sampling.....	4
2.5 Bulk RNA sequencing.....	5
2.5.1 Tissue Preparation and Antigen Retrieval.....	5
2.5.2 VIP Immunohistochemistry (HRP-DAB).....	5
2.5.3 GAP43 Immunohistochemistry (Alkaline Phosphatase–Vector Red)	
6	
2.5.4 Immunostaining optimization.....	7
2.5.5 Negative Controls.....	7
2.6 Blinding and bias control.....	8
2.7 Image analysis and signal quantification.....	8
2.8 Statistical analysis.....	9
3 Results.....	11
3.1 Participant characteristics.....	11
3.2 Transcriptomic guidance for marker selection.....	12
3.3 Comparative analysis of marker mRNA and protein expression.....	12
3.3.1 GAP43 and VIP protein expression in colonic mucosa in relation to	
IBS subtypes or gastroduodenal DGBI overlap.....	12
3.3.2 Marker mRNA and protein expression analysis within IBS.....	16
3.3.3 Marker mRNA and protein expression analysis in IBS stratified by	
DGBI status.....	18
3.4 Distinctive associations of neuronal sprouting and VIP expression with pain	
and visceral sensitivity in IBS.....	19
3.5 Technical validation of quantitative immunohistochemistry.....	23
4 Discussion.....	23
4.1 Overview.....	23
4.2 Neuronal marker selection.....	23
4.3 Methods selection and troubleshooting.....	24
4.4 Homeostatic architecture in healthy controls.....	25
4.5 Layer-specific neuronal remodeling in IBS.....	25
4.5.1 Tendency towards regulatory imbalance in DGBI subgroups.....	27
5 Ethical aspects and research impact.....	30
5.1 Ethical aspects.....	30
5.2 Research impact.....	30
6 Strengths, limitations and future perspectives.....	31
7 References.....	32

Supplementary information.....	38
Declaration of AI and AI-assisted technologies:.....	47

1 Introduction

Disorders of gut–brain interaction (DGBI) are highly prevalent worldwide, affecting up to 40% of people according to a large international study (Sperber et al., 2021). They encompass a spectrum of persistent or recurring gastrointestinal (GI) symptoms that arise without identifiable structural abnormalities, biochemical disturbances, or specific underlying disease (Schmulson & Drossman, 2017). The symptoms are believed to arise from a complex interplay of mechanisms, including disruptions in gut microbiota, modified mucosal immune responses, increased visceral sensitivity, disruption in the gut epithelial and vascular barrier, and dysregulation of central nervous system pathways that affect GI signaling and motility (Drossman et al., 2016; Barbaro et al., 2024)

The most common DGBIs are functional dyspepsia (FD) and irritable bowel syndrome (IBS), which are diagnosed according to the Rome IV criteria (Van den Houste et al., 2021). FD is a common chronic condition, reported by 20% to 30% of the public each year (Talley et al., 1992; Agréus et al., 1995). It is diagnosed in the absence of notable gastric endoscopic findings and without abnormal routine clinical results to account for various symptoms, which may include epigastric pain, burning sensation, early satiation, and postprandial fullness (Tack et al., 2006). IBS is a chronic functional bowel disorder defined by the lack of any colonoscopic abnormalities and normal clinical evaluations, nevertheless accompanied by several gastrointestinal symptoms, notably recurring abdominal pain linked to one or more of the following: alteration in bowel and defecation patterns (constipation, diarrhea, or a combination of both) and abdominal bloating/distension (Mearin et al., 2016). In six studies employing Rome IV criteria across 34 nations (n = 82,476), the summed prevalence of IBS was 3.8% (Oka et al., 2020).

A systematic review and meta-analysis by Lovell and Ford (2012) demonstrated that IBS exhibits a moderately higher prevalence among women compared with men. This pattern remained consistent across diverse geographic regions and diagnostic criteria. Furthermore, gender-related differences were observed in IBS subtypes, with women more frequently presenting with constipation-predominant IBS and more comorbidities, whereas men were more likely to exhibit the diarrhea-predominant subtype (Bureychak et al., 2022).

A characteristic feature of IBS is visceral hypersensitivity, occurring in 20–90% of IBS patients, with 94% of IBS patients reportedly experience altered rectal perception (Mertz et al., 1995). This altered perception is characterized by diminished discomfort thresholds, increased sensation intensity, or unusual viscerosomatic referral (Mertz et al., 1995). However, symptom patterns and mechanisms do not reliably predict sensitivity to rectal distension (Azpiroz et al., 2007).

According to a study done by Tack et al. (2001), visceral hypersensitivity was observed in 34% of FD patients. Patients were hypersensitive to gastric distention, despite similar demographic and pathophysiology features. Hypersensitivity to distention increased postprandial discomfort, belching, and weight loss.

IBS and functional dyspepsia showed a gradual increase in GI symptom severity with increased GI visceral sensitivity across numerous large patient groups from different countries, different sensitivity methodologies, and different GI tract assessments (Simrén et al., 2018). These findings show that visceral hypersensitivity promotes DGBI GI symptoms.

Visceral hypersensitivity is believed to stem from both central nervous system and peripheral mechanisms (Dothel et al., 2015). Neuroplasticity in the IBS mucosa is characterized by increased nerve fiber density and sprouting (Fujikawa & Tominaga, 2023). Mucosal mediators from IBS samples boosted neuron growth factor-dependent neurite outgrowth in mouse enteric and human SH-SY5Y neurons (Dothel et al., 2015). Another study in rat IBS models revealed a significant enhancement of the mucosal and submucosal neural networks, along with mucosal neuronal outgrowth, suggesting increased expression of neurotrophic factors that facilitate neuronal sprouting (Fujikawa & Tominaga, 2023).

Previous RNA-Seq and RT-PCR investigations of the rectosigmoid mucosa in IBS with predominant diarrhea (IBS-D) revealed transcriptome changes affecting neurotransmitters, ion channels, cytokines, immunological functions, cell adhesion, and barrier integrity. Interestingly, upregulated genes included a number of nerve markers (Camilleri et al., 2014). Research on guinea pigs demonstrated that the intestinal myenteric plexus possesses regenerative capabilities following transection (Galligan et al., 1989), thereby confirming that the enteric nervous system (ENS) exhibits both regenerative and sprouting potential.

Taken together, this indicates that IBS is associated with neuronal changes at the mucosal level that may be detected through changes in intestinal neuropeptide expression. For instance, the neuropeptide vasoactive intestinal polypeptide (VIP) was found to be doubled in IBS patients compared to healthy controls in a study using rectal biopsies (Palsson et al., 2004). However, whether these mechanisms are affected by the presence of other, concomitant DGBI remains unknown.

Studies have shown that while many individuals with DGBI experience symptoms in only one gastrointestinal region (68.3%), a significant proportion have symptoms in two (22.3%), three (7.1%), or all four regions—oesophageal, gastroduodenal, bowel, and anorectal (2.3%) (Sperber et al., 2022), underscoring that symptom overlap is a common feature in DGBI. Aziz et al. (2017) reported that DGBI was identified in around one-third of the general

population, with one-third of this cohort showing overlapping symptoms across multiple gastrointestinal areas. This overlap was associated with increased somatization, reduced mental and physical quality of life, a rise in medical interventions, and a higher frequency of abdominal surgeries relative to individuals with organic gastrointestinal disorders (Aziz et al., 2017).

Several studies summarized by Suzuki and Hibi (2011) show that FD and IBS typically coexist, with clinical overlap increasing disease burden. Individual cases of FD and IBS were often recorded in Rome III-classified population-based and outpatient cohorts, 1–5% of patients had FD–IBS overlap (Suzuki & Hibi, 2011). FD-IBS overlap cause more severe gastrointestinal symptoms, particularly postprandial fullness, and a lower health-related quality of life (Wang et al., 2008; Kaji et al., 2010). FD–IBS overlap was associated with worse mental health outcomes, including higher depressive symptom scores and lower quality of life (Lee et al., 2010), indicating a more severe clinical phenotype rather than a simple coexistence of two DGBIs.

This takes us to the question of whether overlap with other DGBI could define a separate subgroup of IBS with distinctive underlying mechanisms. The specific aims of this project were:

- 1) To compare colonic mucosal neuronal sprouting and VIP protein expression in IBS with and without overlapping gastroduodenal DGBI.
- 2) To compare intestinal and extraintestinal symptoms in IBS with and without overlapping gastroduodenal DGBI and mucosal neuronal alterations.

2 Materials and Methods

2.1 Study population

Participants with IBS were prospectively recruited during five years (2015–2020) from the neurogastroenterology unit at the Sahlgrenska University Hospital (Gothenburg, Sweden), which is a tertiary clinical center. DGBI were diagnosed according to the Rome IV diagnostic criteria. Asymptomatic volunteers, i.e., persons without any chronic diseases or significant gastrointestinal symptoms, were recruited through advertisements and included as healthy controls.

All patients provided informed consent, and the study was approved by the Ethics Review Board in Gothenburg (988-14).

2.1.1 Inclusion and exclusion criteria

The inclusion criteria were at least 18 years of age at baseline visit and symptoms suggestive of a functional bowel disorder or an established functional bowel disorder. Exclusion criteria were: abnormal results on the screening laboratory tests, clinically relevant for study participation; other gastrointestinal disease(s); other severe disease(s) (i.e., malignancy, severe heart disease, kidney disease or neurological disease); symptoms indicating other severe disease(s) (i.e., gastrointestinal bleeding, weight loss or fever); severe psychiatric disease; previous history of alcohol abuse; consumption of antibiotics one month previous to the screening and throughout the study; consumption of cortisone, non-steroidal anti-inflammatory drugs or other anti-inflammatory drugs on a regular basis two weeks prior to screening and throughout the study; pregnant or lactating or wish to become pregnant during the period of the study.

2.2 Symptom Questionnaires

Each subject completed a series of questionnaires to assess gastrointestinal symptom severity and psychological comorbidities. Gastrointestinal symptoms were quantified using the Gastrointestinal Symptom Rating Scale (GSRS) (Svedlund et al., 1988). Anxiety and depression were assessed using the Hospital Anxiety and Depression Scale (HADS) (Zigmond et al., 1983), which provides separate scores for anxiety (HAD-A) and depression (HAD-D).

2.3 Assessment of visceral sensitivity

A rectal barostat measured visceral sensation. This is a reliable standardized technique that applies regulated, mechanical rectum distensions to assess visceral sensitivity (Whitehead et al., 1990). A barostat system, which contains a flexible polyethylene balloon connected to a computerized pressure-regulated device, does the exact pressure regulation, regardless of the rectal tone. Before testing, the deflated balloon was inserted in the rectum and allowed to reach its normal working pressure. Next, pressure was slowly raised at set times to make the area expand. At each pressure step, participants were told to use conventional descriptions to describe how they felt. The pressure at which the initial sensation of distension occurred and the pressure that induced discomfort or pain were documented. Adequate rest periods were put between distensions intervals to avoid sensitivity or adaptation.

2.4 Sigmoidoscopy and biopsy sampling

During a partial colonoscopy (sigmoidoscopy), mucosal biopsies were taken from the sigmoid colon, 20 cm from the anal verge, and used for bulk RNA sequencing, histology and immunohistochemistry.

2.5 Bulk RNA sequencing

Bulk RNA sequencing of colonic mucosal biopsies and library preparation were conducted prior the present study within the same research group, using the same patient cohort, to characterize molecular alterations associated with disorders of gut–brain interaction. The processed RNA-seq dataset was made available at the start of this project. In the present study, downstream analysis of the RNA-seq data was conducted, and significantly differentially expressed genes were shortlisted based on neuronal relevance, colocalization potential, nerve specificity, spatial protein localization, and expression patterns across distinct layers of the colonic wall.

RNA was extracted from whole biopsies from sigmoid colon using RNeasy Mini kit (Qiagen, #74106). Isolated RNA quality was confirmed using a Bioanalyzer (Agilent) with RIN value greater than 8. Preparation of cDNA libraries was done using the TrueSeqstranded Total RNA Sample Preparation kit with Ribo-Zero Plus (Illumina) according to manufacturer's protocol and sequenced thereafter via paired-end with the NovaSeq 6000 platform (Illumina). Quality of the sequencing was measured for all lanes, reads and cycles with 93.45% of bases above Q30. The quality of raw reads was assessed using FastQC (version 0.11.2) evaluating for per base sequence quality and adaptor contamination. The reads were mapped against the human transcriptome, release 38 (GRCh38.p13) from Gencode using Salmon (version 1.10.1) (Frankish et al., 2023). The expression levels of each gene were calculated as transcripts per million (TPM) using R library tximport (v1.18.0) (Soneson et al., 2015). The read counts were quantified and normalized by the median of ratio method via the R package DESeq2 (v1.30.1) (Michael et al., 2014).

2.5.1 Tissue Preparation and Antigen Retrieval

Formalin-fixed, paraffin-embedded colonic biopsy sections were cut at 5 μm , mounted on glass slides, and dried. Sections were deparaffinized with xylene (two immersions at 5 min each) and rehydrated through graded ethanol (100%, 95%, and 70%, 3 min each), followed by rinsing in running tap water for 3 min. Slides were not allowed to dry at any stage.

Heat-induced epitope retrieval was performed by immersing sections in high-pH antigen retrieval buffer (IHC Antigen Retrieval Solution, 10 \times , Invitrogen, Thermo Fisher Scientific; Cat. No. 00-4956-58) using a pressure cooker system (2100 Retriever). Slides were allowed to cool at room temperature before further processing. All incubations were performed in a humidified chamber.

2.5.2 VIP Immunohistochemistry (HRP-DAB)

After antigen retrieval, sections were washed for 5 min in Tris-buffered saline containing 0.05% Tween-20 (TBST, pH 7.4). Endogenous peroxidase activity

was quenched by incubation in 3% hydrogen peroxide in TBS for 10 min at room temperature, followed by two 5-min washes in TBST.

Non-specific binding was blocked using 5% normal goat serum (Vector Laboratories, Inc.; REF S-1000, Lot ZL0510) diluted in TBS for 20 min at room temperature.

Sections were incubated overnight at 4 °C with rabbit anti-VIP primary antibody (Proteintech; Catalog No. 16233-1-AP, Lot 00041691) diluted 1:1500 in TBS.

After two 5-min washes in TBST, sections were incubated for 30 min at room temperature with biotinylated goat anti-rabbit IgG (H+L) (Vector Laboratories, Inc.; REF BA-1000, Lot ZL0606) diluted 1:200 in TBS.

Following two 10-min washes in TBST, sections were incubated for 60 min at room temperature with VECTASTAIN® ABC Peroxidase reagent (Vector Laboratories; REF PK-4000, Lot ZL0612). The ABC working solution was prepared fresh 30 min before use by mixing 10 µL Reagent A and 10 µL Reagent B in TBS to a final volume of 1 mL.

Sections underwent two 10-min washes in TBST, then immunoreactivity was visualized using 3,3'-diaminobenzidine (DAB) (Sigma). The working DAB solution contained 0.05% DAB and 0.015% H₂O₂ in 0.01 M PBS (pH 7.2), prepared by diluting aliquots of 1% DAB and 0.3% H₂O₂ stock solutions. Sections were developed for 1–3 min in the dark, with reaction progress monitoring. The reaction was stopped by rinsing in tap water.

Sections were counterstained with Gill's haematoxylin No. 3 (Sigma, GHS316-500ML) for 45 s, rinsed thoroughly in running water, briefly dipped twice in 0.25% ammonia water, and rinsed thoroughly again. Slides were dehydrated through graded ethanol (70%, 95%, and 100%), cleared in 2 xylene changes, all steps for 5 min each, and mounted with permanent mounting medium.

2.5.3 GAP43 Immunohistochemistry (Alkaline Phosphatase–Vector Red)

After antigen retrieval, sections underwent two washing steps in TBS (pH 7.4) 5 min each. Non-specific binding was blocked using 2.5% normal horse serum, supplied within the ImmPRESS®-AP Horse Anti-Mouse IgG Polymer Detection Kit (Vector Laboratories, Inc.; REF MP-5402-15, Cat. No. MP-5402, Lot WOVUS29109), for 20 min at room temperature.

Sections were incubated overnight at 4 °C with mouse monoclonal anti-GAP43 antibody (Novus Biologicals, a Bio-Techne brand; Item No. NBP3-05535-100µL, Lot 062425) diluted 1:500 in TBS.

After two 5-min washes in TBST, sections were incubated for 30 min at room temperature with the ImmPRESS®-AP Horse Anti-Mouse IgG Polymer secondary antibody (Vector Laboratories; REF MP-5402-15). All alkaline

phosphatase (AP) steps were performed using TBS rather than PBS, as phosphate ions inhibit AP activity.

After two 5-min washes in TBST, chromogenic detection was performed using the Vector® Red Alkaline Phosphatase Substrate Kit (Vector Laboratories; REF SK-5100, Lot WO47636). The working solution was prepared fresh, steps according to company provided user guide, in 100 mM Tris-HCl buffer (pH 8.2) containing 0.1% Tween-20. To suppress endogenous alkaline phosphatase activity, levamisole solution (Vector Laboratories; REF SP-5000-18, Lot WOVUS27966) was added at one drop per 5 mL of substrate buffer prior to addition of substrate reagents. Slides were incubated in the dark for 20–30 min, with reaction development monitoring.

Sections were rinsed in tap water and counterstained with Gill's haematoxylin No. 3 for 45 s, followed by rinsing in running water and brief two times immersion in 0.25% ammonia water. Slides were washed thoroughly, dehydrated through graded ethanol, cleared in xylene, and mounted permanently.

2.5.4 Immunostaining optimization

During method development, immunofluorescence-based immunohistochemical (IF-IHC) colocalization of VIP and GAP43 was initially attempted to visualize neuronal markers within the same tissue section. However, VIP immunofluorescence consistently produced a diffuse, punctate “starry sky” pattern that did not colocalize with GAP43 and did not correspond to known enteric neuronal morphology, despite repeated optimization trials. Several VIP primary antibody concentrations were tested without improvement in signal specificity.

To ensure reliable and interpretable quantification, the study was therefore transitioned to a colorimetric immunohistochemistry approach. A pilot colocalization experiment using dual chromogenic detection (VIP with DAB and GAP43 with Vector Red) showed that neuronal profiles were distinctly labeled by either VIP or GAP43, but the overlapping signal density was insufficient for reliable quantitative colocalization. Due to time constraints and to preserve analytical rigor, VIP and GAP43 were subsequently quantified using separate single-stain protocols on duplicate sections from the same participant cohort.

2.5.5 Negative Controls

To confirm staining specificity, negative control sections were done in parallel for both VIP and GAP43 immunohistochemistry. These sections underwent identical steps, including antigen retrieval, blocking, secondary antibody incubation, and chromogenic development, except that the primary antibody was omitted and replaced with TBS. No specific staining was observed in these control sections, confirming that the detected signals in experimental samples

were due to specific binding of the VIP and GAP43 antibodies rather than non-specific background or endogenous enzyme activity.

2.6 Blinding and bias control

To minimize observer bias during staining, imaging, and quantitative analysis, a blinding procedure was implemented at the level of slide identification. Although original sample identifiers were present during sectioning and staining, the large number of samples and the involvement of multiple personnel ensured that the investigator performing the staining was not aware of the clinical group assignment (IBS vs healthy control) of individual specimens. Staining was performed jointly by the author and a team member who likewise had no access to clinical information.

After completion of IHC staining for the full cohort (40 samples stained for VIP and 40 samples stained for GAP43), all slides were anonymized by an independent research nurse. The original sample identifiers were covered with tape and replaced with new numerical codes (1–40) separately for the VIP and GAP43 series, such that the same biological sample received different blinded numbers in the two stains (e.g., a given sample might be coded as “1” in the VIP set and “32” in the GAP43 set). The key linking blinded codes to sample identities was kept by the research nurse and was not released until after all image acquisition, ROI annotation, and QuPath-based quantitative analysis had been completed.

All image selection, region-of-interest annotation, background correction, and optical density quantification were therefore performed in a fully blinded manner with respect to diagnosis, subgroup, and clinical metadata, ensuring that group differences could not influence measurement or analysis.

2.7 Image analysis and signal quantification

Histological images were acquired using a Zeiss Axioplan 2 light microscope equipped with a digital camera and AxioVision software (AxioVs40, version 4.8.2.0; Carl Zeiss Vision). All images were captured at 40× objective magnification using identical hardware and software settings across all samples. The spatial calibration at this magnification was 0.26 μm per pixel and stain vectors were fixed across images for each chromogen quantification.

For each patient sample, four non-overlapping fields of view were collected, comprising two images from the mucosal layer and two images from the muscularis mucosa layer. Fields were selected to include well-preserved tissue architecture and to minimize folds, tears, or staining artifacts. All images were acquired using fixed illumination, exposure, and color balance settings to ensure quantitative comparability across samples.

Regions of interest (ROIs) were manually annotated in QuPath (version 0.6.0) (Bankhead et al., 2017) to correspond to histologically defined compartments of the colonic wall. Crypt epithelium, lamina propria, mucosa (epithelium + lamina propria), and muscularis mucosa were annotated separately based on morphological criteria to enable compartment-specific analysis of VIP/ GAP43 immunoreactivity.

To account for depth-dependent heterogeneity of neuronal marker expression and variable biopsy thickness, muscularis mucosa quantification was restricted to a standardized depth window extending up to 50 μm from the mucosa–muscularis interface. Samples with thinner muscularis mucosa were analysed using the entire available thickness, while deeper regions beyond 50 μm were excluded from analysis. 4 samples lacking identifiable muscularis mucosa were excluded from muscularis-specific analyses.

Occasional nonspecific stain precipitates were excluded from analysis by manually annotating and subtracting small regions from the parent ROIs prior to intensity measurement.

Low-level nonspecific chromogen signal was occasionally observed in goblet cells within crypt epithelium; therefore, background optical density measured in morphologically negative regions was subtracted from all measurements prior to analysis.

Background-subtracted values occasionally yielded negative optical density values, reflecting the absence of specific chromogen signal in those regions.

Signal intensity was measured by QuPath as mean pixel intensity of the stained channel for all detected tissue pixels within each ROI. Following colour deconvolution, the stained channel was used to measure optical density (OD) at the pixel level, where each pixel is assigned an optical density value in absorbance units (AU) based on the Beer–Lambert relationship between transmitted light and stain concentration.

To adjust for tissue size difference in annotated ROIs, the total signal was averaged to the marked tissue area. So, the reported values show the average staining intensity per unit surface area, which is found by adding up the pixel intensities and dividing by the total ROI area (μm^2) giving a measurement of mean optical density per unit area ($\text{AU}/\mu\text{m}^2$). This method gives a quantitative estimate of how much protein or marker there is, regardless of the size of the sample, and it can be compared directly between samples.

For each patient, mean chromogen (DAB or Red substrate) OD values were averaged across multiple images per tissue compartment to obtain a single patient-level value for statistical analysis.

2.8 Statistical analysis

All statistical analyses and data visualization were performed using RStudio (*RStudio 2025.09.0+387 “Cucumberleaf Sunflower” for Windows; R version 4.5.0 (2025-04-11 ucrt) compatible with Quarto 1.7.32*). Clinical variables, transcriptomic data, and quantitative immunohistochemistry measurements

were integrated into a single analysis dataset and analyzed using the tidyverse, rstatix, and ggplot2 packages.

Because most variables did not follow a normal distribution, non-parametric statistical methods were used throughout. Spearman rank correlation was applied to evaluate associations between protein expression of VIP and GAP43 and their corresponding mRNA abundance, between protein expression and abdominal pain scores, and between protein expression and barostat-derived visceral sensitivity measures including first sensation and discomfort thresholds.

Wilcoxon rank-sum tests were used for two-group comparisons such as IBS versus healthy controls, DGBI overlap status, and sex, while Kruskal–Wallis tests were used to compare IBS subtypes (IBS-C, IBS-D, and IBS-M), with post hoc testing performed where appropriate.

Correlations and group comparisons were primarily performed within the IBS cohort, unless explicitly stated otherwise (e.g., IBS vs healthy control comparisons), to avoid dilution of disease-specific effects by healthy subjects.

Results are reported as Spearman correlation coefficients (r) with corresponding p -values, or as test statistics with p -values for group comparisons. A two-sided $p < 0.05$ was considered statistically significant.

3 Results

3.1 Participant characteristics

The study cohort comprised 40 participants, including 8 healthy controls (HC) and 32 patients with IBS, of whom 16 had IBS with gastroduodenal DGBI overlap (IBS_DGBI) and 16 had IBS without overlap (IBS_noDGBI). As summarized in Table 1, sex distribution across groups was as following: 50% of HC were female, compared with 68.8% of the IBS_DGBI group and 81.2% of the IBS_noDGBI group.

Clinical symptom severity and visceral sensitivity differed between HC and IBS groups (Table 1). Mean abdominal pain scores were minimal in HC (1.00 ± 0.00) but markedly elevated in IBS, both in IBS_DGBI (5.09 ± 0.28) and IBS_noDGBI (4.75 ± 0.35). Rectal barostat testing exhibited significant differences in mean visceral sensitivity, with HC exhibiting higher first sensation volumes (77.5 ± 16.2 mL) compared with IBS_DGBI (48.8 ± 5.5 mL) and IBS_noDGBI (52.5 ± 5.3 mL). Similarly, discomfort thresholds were highest in HC (173.1 ± 25.8 mL) and reduced in IBS patients, particularly in those with DGBI overlap (153.8 ± 26.6 mL) and those without overlap (145.0 ± 14.5 mL).

Table 1. Cohort distribution and clinical outcome

Variable	HC	IBS_DGBI	IBS_noDGBI
Abdominal_pain	1.00 ± 0.00	5.09 ± 0.28	4.75 ± 0.35
Baro_discomfort_ml	173.12 ± 25.82	153.75 ± 26.55	145.00 ± 14.49
Baro_firstsens_ml	77.50 ± 16.23	48.75 ± 5.54	52.50 ± 5.28
Gender: Female	4 (50%)	11 (68.8%)	13 (81.2%)
Gender: Male	4 (50%)	5 (31.2%)	3 (18.8%)
Participants number	8 (20%)	16 (40%)	16 (40%)
IBS_subgroups	--	9 IBS-D (56%) 6 IBS-C (38%) 1 IBS-M (6%)	5 IBS-D (31%) 11 IBS-C(69%)

Together, these data indicate that IBS is associated with increased abdominal pain and heightened visceral sensitivity relative to healthy controls, with generally similar symptom severity across IBS subgroups stratified by gastroduodenal DGBI overlap.

3.2 Transcriptomic guidance for marker selection

Bulk RNA sequencing (RNA-seq) pathway-level analysis revealed significant enrichment of genes related to neuronal development, axon guidance, and neurite outgrowth in IBS with overlapping gastroduodenal DGBI compared to IBS patients without this overlap (unpublished data).

Based on these transcriptomic findings, two neuronal markers were selected for protein-level validation in the present study: GAP43 ($\log_2FC = 0.9$, $p < 0.001$, $q = 0.2$ for the comparison of IBS with vs. without overlap with gastroduodenal DGBI, Mann-Whitney U-test) and VIP ($\log_2FC = 0.8$, $p < 0.001$, $q = 0.2$). These markers were among the most significantly altered neuronal genes in the RNA-seq dataset and were chosen to represent different aspects of neuronal remodeling.

Because bulk mucosal RNA-seq reflects mixed cell populations rather than spatially resolved neuronal compartments, transcript levels were used only for technical validation of protein measurements and not for direct correlation with clinical phenotypes.

3.3 Comparative analysis of marker mRNA and protein expression

Quantitative immunohistochemistry demonstrated marked layer-specific neuronal remodeling in IBS. To illustrate the anatomical distribution of neuronal markers, representative images of GAP43 and VIP immunoreactivity across colonic layers are shown in Figure 1.

3.3.1 GAP43 and VIP protein expression in colonic mucosa in relation to IBS subtypes or gastroduodenal DGBI overlap

To determine whether gastroduodenal DGBI overlap is associated with altered VIPergic or GAP43-positive innervation, VIP and GAP43 protein expression was compared across all four mucosal compartments (crypts, lamina propria, mucosa, and muscularis mucosa) among three biological groups: healthy controls (HC), IBS without gastroduodenal DGBI (IBS_noDGBI), and IBS with gastroduodenal DGBI overlap (IBS_DGBI). As shown in Figure 2, which displays box-and-jitter plots of optical density for each marker across all four layers, there were no significant differences in VIP protein expression between HC, IBS_noDGBI, and IBS_DGBI groups in any compartment (all p values > 0.09). Likewise, GAP43 protein levels did not differ significantly between three groups in any layer (Kruskal Wallis test was done with Wilcoxon pairwise comparisons for statistical analysis. All p values > 0.4).

Similarly, no significant differences were observed between healthy controls and IBS subtypes (IBS-C, IBS-D) for either marker in any layer (all $p > 0.15$) (Figure 3). In IBS subtypes, there is one single IBS-M participant out of all the

32 IBS cohort, so it was omitted from the comparison as to not invalidate the correlation. These findings indicate that neuronal remodeling in IBS is not defined by absolute increases in neuronal marker expression but rather by how layer-specific neuronal phenotypes relate to visceral sensitivity and pain.

These findings demonstrate that in this study, gastroduodenal DGBI subgroups are not associated with a change in the absolute density of VIPergic or GAP43-positive fibers compared to the healthy condition.

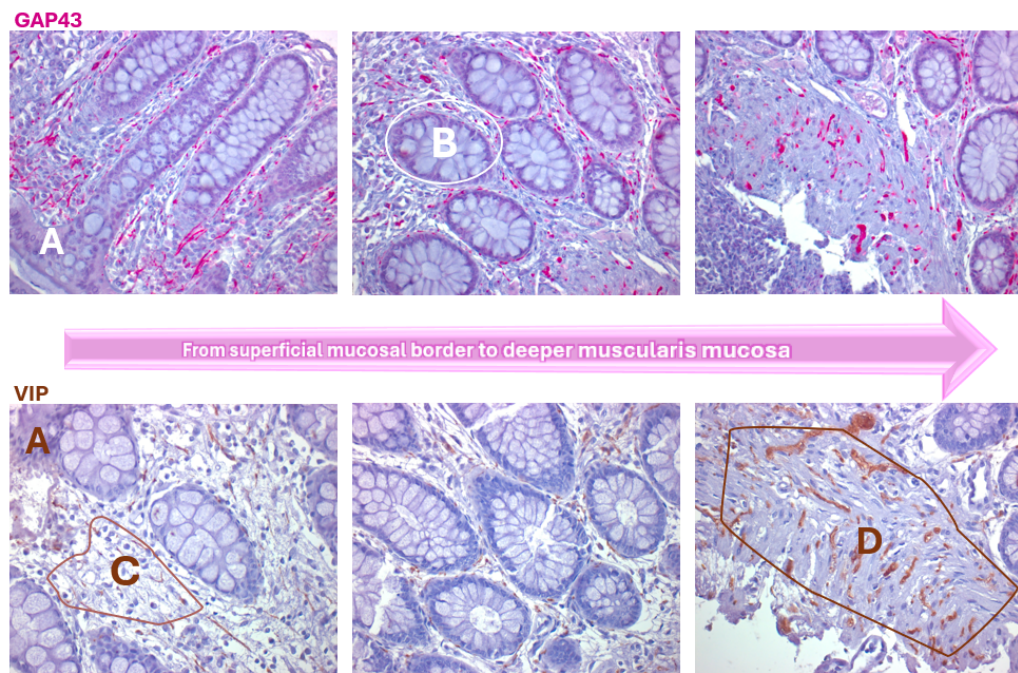


Figure 1 Layer-specific distribution of neuronal markers in the colonic wall. Representative immunohistochemical staining for GAP43 (upper row, red chromogen) and VIP (lower row, brown DAB) in colonic biopsies from IBS patients. Panels, at 40x magnification, illustrate progressively deeper tissue layers from the superficial epithelium toward the muscularis mucosa. (A) Surface epithelium, (B) crypt epithelium, (C) lamina propria, and (D) muscularis mucosae.

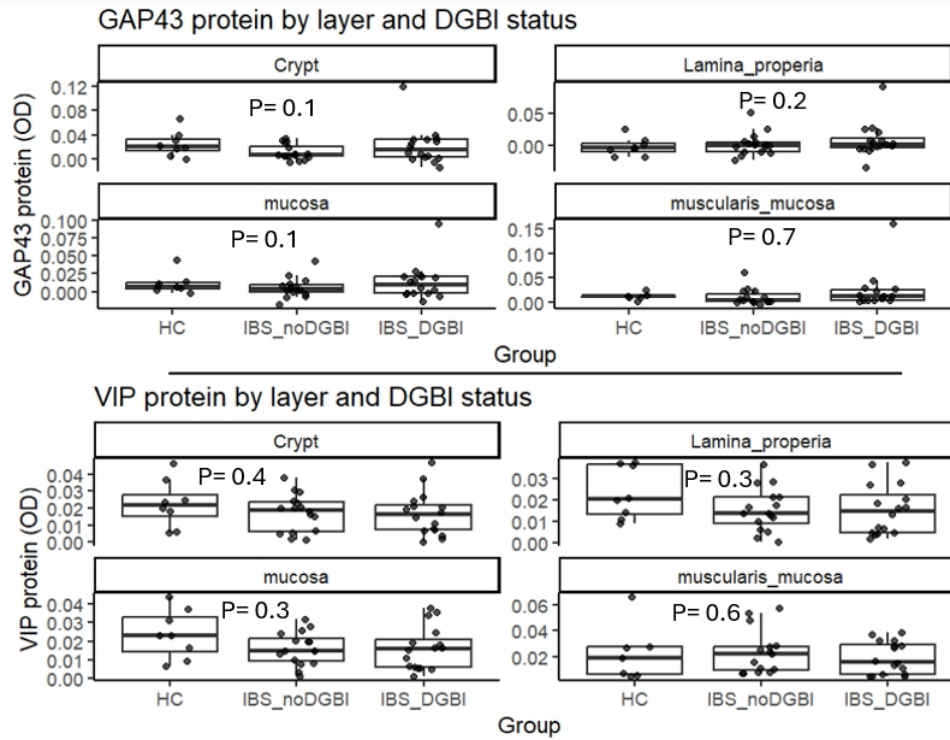


Figure 2 Comparison between VIP and GAP43 OD protein expression across all four mucosal compartments among HC and IBS groups stratified by gastroduodenal DGBI overlap status. Kruskal Wallis test was done with Wilcoxon pairwise comparisons for statistical analysis

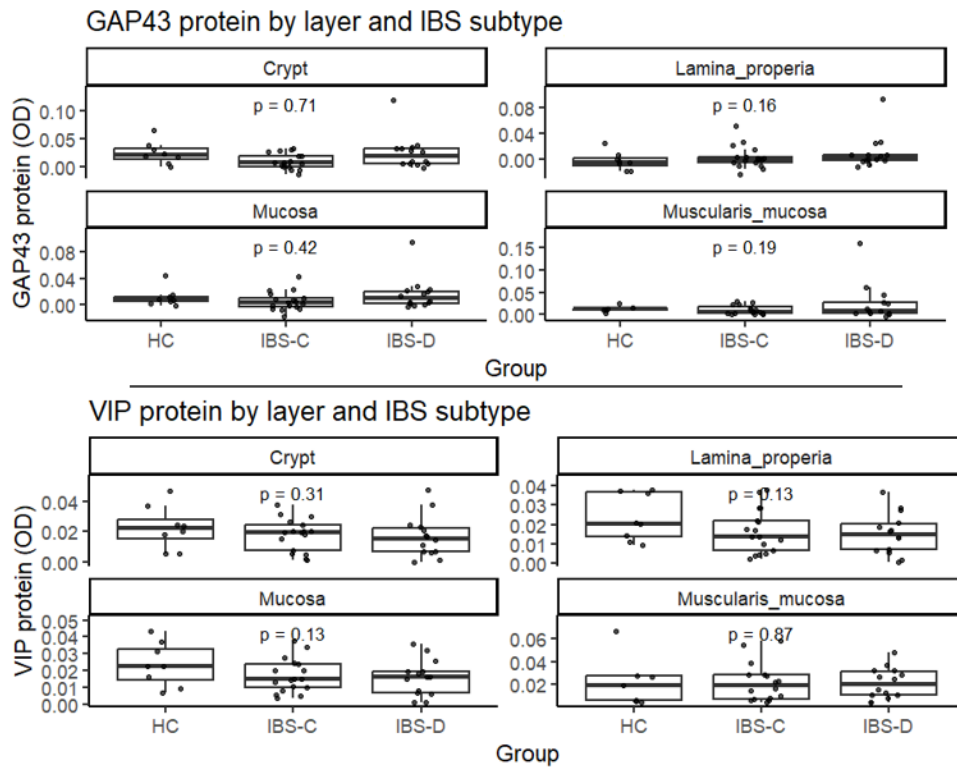


Figure 3 Comparison between VIP and GAP43 OD protein expression across all four

mucosal compartments among HC and IBS groups, stratified by bowel movement habits into IBS constipation (IBS-C) and IBS diarrhea (IBS-D). Kruskal Wallis test was done with Wilcoxon pairwise comparisons for statistical analysis

Within the IBS cohort, VIP protein levels showed a strong correlation across all mucosal compartments within the same marker (Spearman ρ I = 0.42-0.94, all $p < 0.02$). Likewise, GAP43 protein levels showed same strong positive correlation ($r = 0.54-0.81$, all $p < 0.003$), which proves a compartment-spanning signal and global neuronal plasticity rather than isolated compartment changes (Supplementary Table S1).

Similarly, In the healthy controls VIP protein levels showed strong positive correlations within the same marker across the vertical mucosal axis, with significant associations between crypt and lamina propria, crypt and mucosa, crypt and muscularis mucosa, and between mucosa and lamina propria (all $p < 0.05$). Two additional VIP layer pairs demonstrated trend-level correlations ($0.05 < p < 0.07$), consistent with limited power in the HC subgroup ($n = 8$) rather than absence of biological coupling. In contrast, GAP43, a marker of axonal growth and remodeling, showed minimal inter-layer coupling in HC, with only a weak trend-level association between crypt and mucosal expression ($0.05 < p < 0.07$) and no other significant correlations (Supplementary Table S1).

These HC data define the physiological baseline against which disease-associated alterations in layer-specific neuroplasticity were interpreted.

3.3.2 Marker mRNA and protein expression analysis within IBS

To capture any disease specific remodelling, comparisons were made within the collective IBS cohort first. In the muscularis mucosa, GAP43 muscularis mucosa immunoreactivity correlated with VIP mRNA expression ($r = 0.42$, $p = 0.023$; *Figure 4A*). Similarly, GAP43 muscularis mucosa immunoreactivity correlated with GAP43 mRNA expression ($r = 0.41$, $p = 0.025$; *Figure 4B*), consistent with this layer reflecting structural enteric neuronal density. No significant correlations were observed between GAP43 mRNA levels and protein expression for the other compartments (Table 2). and no other significant correlations were observed between VIP mRNA levels and protein expression for the other compartments (Table 3).

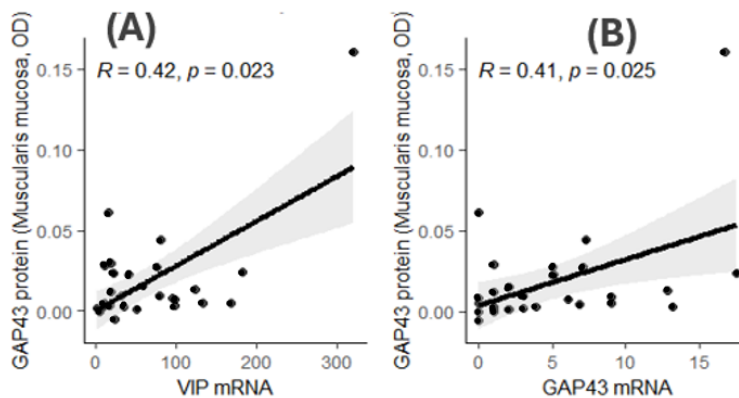


Figure 4 VIP-GAP43 coupling. Each dot represents an IBS participant. Graph (A) shows relationship between VIP normalized mRNA expression, and GAP43 immunoreactivity in the muscularis mucosa, quantified as background-subtracted mean RED optical density (OD, AU). VIP mRNA correlates positively with GAP43 OD ($r = 0.42$, $p = 0.023$). Graph (B) shows a significant correlation between GAP43 OD within muscularis ROIs and GAP43 normalized mRNA transcript levels ($r = 0.41$, $p = 0.025$). R is the Spearman correlation coefficient.

Cross-layer analysis showed that VIP-positive fibers and GAP43-positive fibers were not related to each other. In HC there were no observed correlations in protein expression between the two markers (Supplementary Table S5). There was a negative correlation between GAP43 expression in the lamina propria and VIP immunoreactivity in the mucosa ($r = -0.35$, $p = 0.046$; *Figure 5*). This means that when nerve fibers sprout more in immune-rich areas, VIP signaling at the epithelial interface goes down. This was the only significant correlation observed within the combined IBS cohort between VIP and GAP43 positive fibers across all compartments (Supplementary Table S7).

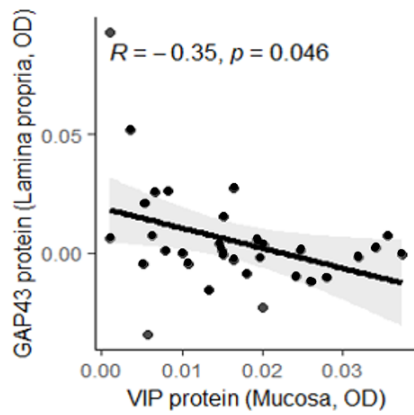


Figure 5 Correlation within IBS between GAP 43 lamina propria immunoreactivity and VIP mucosa immunoreactivity showing inverse correlation ($r = -0.35$, $p = 0.046$). Each dot signifies an individual participant. R is the Spearman correlation coefficient.

Table 2 Correlation in IBS between expression of protein across layers and GAP43 mRNA

Protein layer OD	GAP43 mRNA	r	p
GAP43_muscularis_mucosa	GAP43	0.4100	0.02490
VIP_Crypt	GAP43	0.1700	0.34800
GAP43_Crypt	GAP43	0.1700	0.35600
GAP43_Lamina_properia	GAP43	0.1500	0.40000
GAP43_mucosa	GAP43	0.0470	0.79700
VIP_muscularis_mucosa	GAP43	-0.1000	0.58400
VIP_mucosa	GAP43	-0.1000	0.57600
VIP_Lamina_properia	GAP43	-0.1700	0.36300

Table 3 Correlation in IBS between expression of protein across layers and VIP mRNA

Protein layer OD	VIP mRNA	r	p
GAP43_muscularis_mucosa	VIP	0.4200	0.02300
GAP43_Crypt	VIP	0.1700	0.33700
VIP_muscularis_mucosa	VIP	0.0052	0.97800
GAP43_Lamina_properia	VIP	0.0890	0.62700
GAP43_mucosa	VIP	0.0620	0.73700
VIP_Crypt	VIP	-0.0190	0.91800
VIP_mucosa	VIP	-0.1800	0.32700
VIP_Lamina_properia	VIP	-0.2100	0.24800

3.3.3 Marker mRNA and protein expression analysis in IBS stratified by DGBI status

Further relationships within DGBI subtypes were explored to determine whether VIP and GAP43 protein and transcriptomic expression were differentially distributed across anatomical layers of colonic wall.

Within the DGBI non-overlap subgroup, GAP43 protein in the lamina propria showed a significant inverse relationship with VIP protein in lamina propria ($r = -0.64$, $p = 0.0086$, Figure 6A), indicating that greater lamina propria-based nerve sprouting was associated with reduced local VIP protein abundance. A parallel inverse association was also observed between GAP43 protein in the lamina propria and VIP protein in the mucosa ($r = -0.6$, $p = 0.015$, Figure 6B), revealing a coherent decoupling between VIP transcriptional and protein localization. Interestingly, this significant negative correlation was not observed in the IBS overlap subgroup, which indicates that the inverse correlation between VIP and GAP43 immunoreactivity across compartments is driven more by the gastroduodenal non-overlap subgroup of IBS (Supplementary Tables, Table S8 & Table S9). Yet on the transcriptomic-protein level, there were no significant correlations observed across any of the anatomical compartments for this IBS subgroup (Supplementary Table S5)

However, within the DGBI overlap subgroup, a specific mode of dissociation was observed at the transcriptional-anatomical level: VIP mRNA was inversely correlated with VIP protein expression in the lamina propria ($r = -0.52$, $p = 0.042$, Figure 6C), and no other significant correlations were observed within

this subgroup between mRNA transcription and protein expression for the tested markers (Supplementary Table S6)

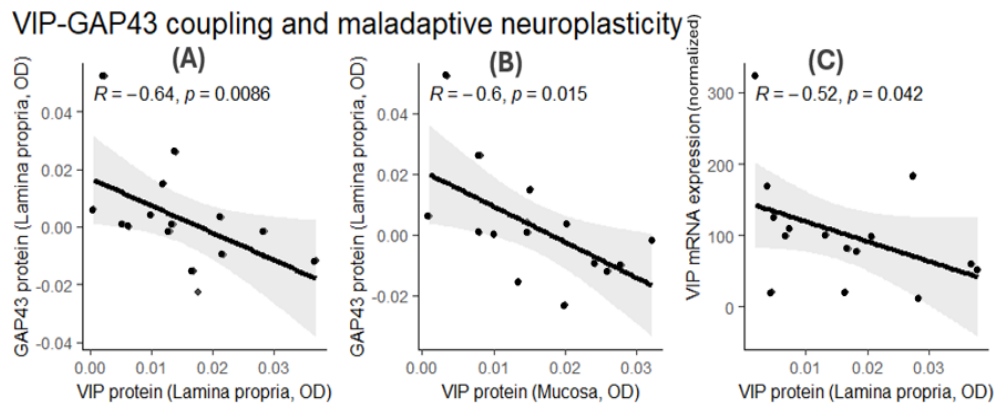


Figure 6. Correlations within layer- and IBS subgroup- with VIP & GAP43 transcription and expression. Each dot signifies an individual participant. Graph (A) showing that In the IBS non-overlap subgroup, GAP43 protein expression in the lamina propria, quantified as background-subtracted mean RED optical density (OD, AU), is inversely correlated with VIP protein expression in the lamina propria, quantified as background-subtracted mean DAB OD (AU) ($r = -0.64$, $p = 0.0086$). Graph (B) showing also in IBS non-overlap, GAP43 protein in the lamina propria is inversely correlated with VIP protein in the mucosa ($r = -0.6$, $p = 0.015$). In contrast, graph (C) shows that within DGBI overlap IBS subgroups, VIP mRNA normalized expression is inversely correlated with VIP protein levels in the lamina propria ($r = -0.52$, $p = 0.042$). R is the Spearman correlation coefficient.

3.4 Distinctive associations of neuronal sprouting and VIP expression with pain and visceral sensitivity in IBS

In the combined IBS cohort, VIP expression in the muscularis mucosa showed a trend-level inverse relationship with rectal discomfort thresholds ($r = -0.33$, $p = 0.068$; *Figure 7A*), suggesting that increased VIP expression may be linked to visceral hypersensitivity.

Conversely, GAP43 immunoreactivity in the crypt adjacent mucosa showed a trend inverse correlation with abdominal pain severity ($r = -0.38$, $p = 0.034$; *Figure 7B*), with a similar but stronger association observed in the lamina propria ($r = -0.49$, $p = 0.0047$; *Figure 7C*), indicating that mucosal nerve fiber sprouting may be linked to symptom improvement. In contrast, GAP43 expression was not significantly associated with visceral sensitivity. These relationships were interestingly more prominent within IBS subgroups. In

gastroduodenal DGBI overlap subgroup, abdominal pain inversely correlated with GAP43 immunoreactivity in all three compartments; lamina propria ($r = -0.58$, $p = 0.02$; *Figure 8A*), mucosa ($r = -0.49$, $p = 0.054$; *Figure 8B*) and muscularis mucosa ($r = -0.47$, $p = 0.076$; *Figure 8C*).

While in DGBI non-overlap, the only significant correlation was a positive one between VIP muscularis mucosa and abdominal pain ($r = 0.59$, $p = 0.022$; *Figure 9*).

Which indicates that the inverse correlation between abdominal pain and GAP43 immunoreactivity across compartments is driven more by the gastroduodenal DGBI overlap subgroup of IBS, while in DGBI non-overlap subgroup pain and visceral hypersensitivity seems to be driven from muscularis mucosa VIPergic neuronal activity.

The rest of the clinical symptoms didn't show any other significant correlations or trends with protein expression across compartments in both subgroups of IBS (Supplementary tables, Table S2 & Table S3)

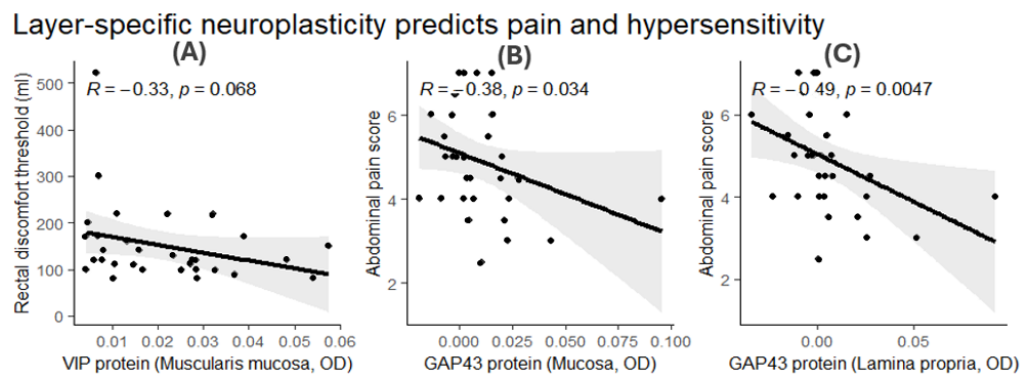


Figure 7. Correlation between GAP43 and VIP immunoreactivity with pain and hypersensitivity in IBS. Each dot signifies an individual participant. Graph (A) illustrates the correlation between VIP background-subtracted mean DAB OD in the muscularis mucosa ROIs and the rectal discomfort threshold assessed using barostat (mL) testing. A higher VIP OD correlates with reduced pain volumes ($r = -0.33$, $p = 0.068$). The correlations between GAP43 background-subtracted RED mean OD and abdominal pain scores are illustrated in Graphs (B) and (C). GAP43 immunoreactivity in mucosal ROIs exhibits an inverse correlation with abdominal pain ($r = -0.38$, $p = 0.034$), while GAP43 immunoreactivity in the lamina propria ROIs shows a significant inverse correlation with abdominal pain scores ($r = -0.49$, $p = 0.0047$). R is the Spearman correlation coefficient.

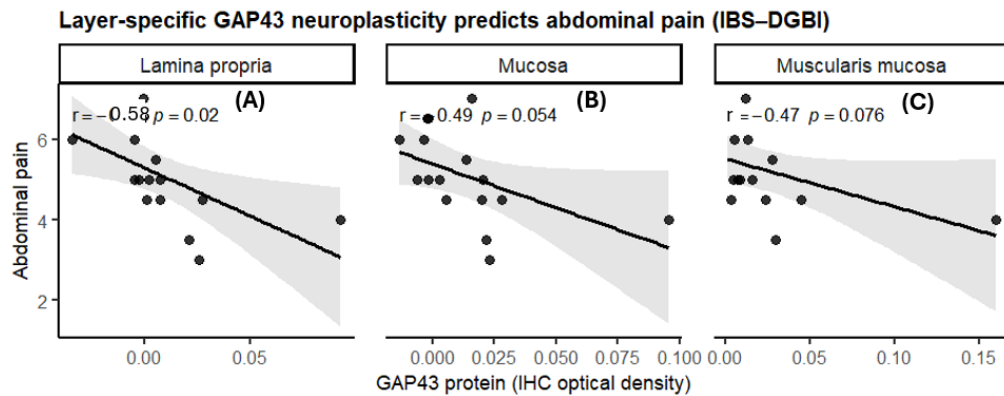


Figure 8 Correlation between GAP43 immunoreactivity across compartments and abdominal pain within gastroduodenal DGBI overlap IBS subgroup, each dot signifies an individual participant. Graph (A) shows GAP43 immunoreactivity in lamina propria ROIs exhibiting an inverse correlation with abdominal pain ($r = -0.58$, $p = 0.02$). Graph (B) shows GAP43 immunoreactivity in the mucosa ROIs shows a significant inverse correlation with abdominal pain scores ($r = -0.49$, $p = 0.054$). Graph (C) showing a trend inverse correlation between immunoreactivity in the muscularis mucosa ROIs with abdominal pain ($r = -0.47$, $p = 0.076$). r is the Spearman correlation coefficient.

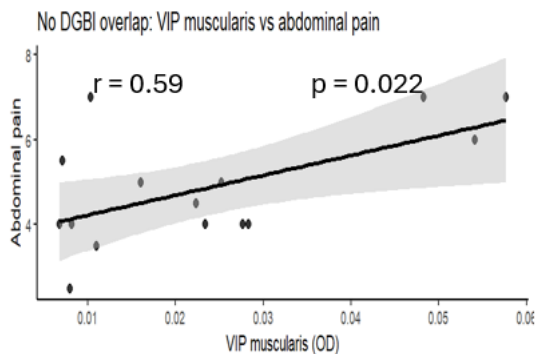


Figure 9 shows correlation within IBS gastroduodenal DGBI non overlap between abdominal pain and VIP immunoreactivity in muscularis mucosa layer. Each dot signifies an individual participant. r is the Spearman correlation coefficient.

Together, these findings support a model in which IBS symptoms may be driven by two complementary forms of neuronal remodeling: mucosal nerve fiber sprouting, reflected by GAP43 and associated with decreased abdominal pain,

and neurochemical phenotypic remodeling of enteric neurons, reflected by VIP within the muscularis mucosa and associated with altered visceral sensitivity.

Observations suggest that IBS may be a disorder of layer-specific neuronal remodelling, integrating structural nerve fibre sprouting with neurochemical programming of enteric neurons (*Figure 10*)

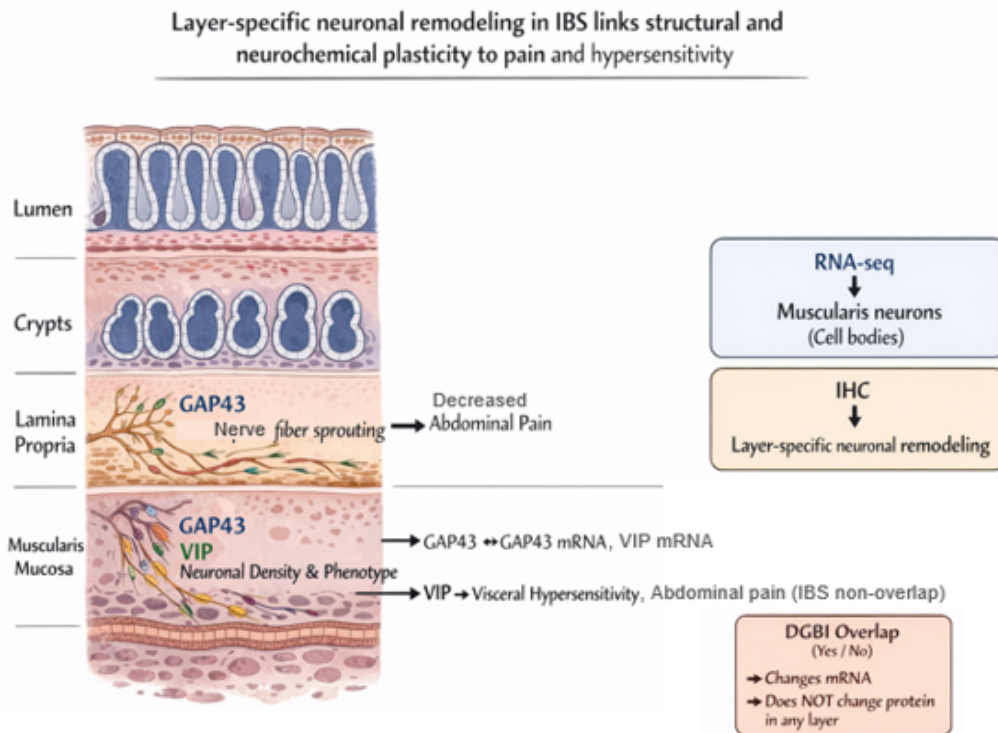


Figure 10 shows the nerve network and its different nerve fiber interactions in the colonic wall. GAP43-positive nerve fiber sprouting in the lamina propria is associated with decreased abdominal pain. Conversely, GAP43 protein positivity in the muscularis mucosa indicates enteric neuronal density and correlates with GAP43 mRNA, but VIP protein expression in these neurons is linked to visceral hypersensitivity in the combined IBS cohort and abdominal pain in IBS non-overlap. Transcriptomic abnormalities related to gastroduodenal DGBI overlap do not result in layer-specific protein alterations, suggesting post-transcriptional and compartment modulation of neuronal activity. (Figure is generated with the help of ChatGPT).

3.5 Technical validation of quantitative immunohistochemistry

To verify the specificity and anatomical precision of the image analysis pipeline, neuronal marker expression was assessed across available histological compartments. Crypt epithelial sections lacked correlation with clinical factors (Supplementary table S2, S3), thereby validating their efficacy as internal negative controls.

In IBS patients, GAP43 immunoreactivity in the muscularis mucosa showed a significant correlation with GAP43 mRNA levels obtained from bulk RNA sequencing (Spearman $r = 0.41$, $p = 0.025$). The transcriptomic and histological data correlation shows that muscularis ROIs are a good way to measure neuronal density.

4 Discussion

4.1 Overview

This study provides layer-resolved, quantitative demonstration that enteric neuronal remodeling in IBS could drive symptoms severity. Combining layer-specific immunohistochemistry with transcriptomic and clinical data showed that instead of simply increasing nerve density, this remodeling is spatially misdirected, producing a shift of neuronal outgrowth away from the mucosal sensory compartment and towards deeper muscularis mucosal layer. This is especially shown in the tendency towards inverse correlations, especially within the DGBI overlap subgroup, between abdominal pain and GAP43 nerve sprouting across all mucosal layers (*Figure 8*). Conversely, in the less severe phenotype of DGBI non-overlap, VIP immunoreactivity in muscularis mucosa positively correlated with abdominal pain (*Figure 9*). This could suggest that, in IBS, stratified by overlapping DGBI subgroups, architectural redistribution predicts visceral hypersensitivity and pain.

4.2 Neuronal marker selection

This study was motivated by transcriptomic data showing differential expression of neuronal development and sprouting pathways across DGBI subgroups.

Markers exhibiting the most robust statistical signals were prioritized, resulting in the selection of VIP and GAP43. These markers were selected due to their neuron specificity, with proteins that are abundantly expressed and spatially positive inside colonic mucosal compartments. The biopsy specimens are limited to the mucosa and muscularis mucosa, seldom extending into the submucosa, which unfortunately impairs visualization of neuronal branching and full architectural visualization since the ENS is deeply located, with

neuronal somata located in the Meissner's plexus in the submucosa and the Auerbach's plexus between the colonic longitudinal and circular deep muscular layers (Uesaka et al., 2016).

Therefore, these observations further underline the importance of finding neuronal axonal markers that are expressed in the superficial mucosal layers.

VIP is a neuropeptide secreted from the noncholinergic secretomotor neurons in the enteric nervous system and acts as a secretomotor neurotransmitter at the neuro-epithelial junction (Banks et al. 2005).

GAP-43 serves as a reliable marker for neuronal sprouting and growth, showing high concentrations at the growth cone plasma membrane (He et al. 1997). It plays a vital role in neuronal growth, axonal pathfinding, and synaptic plasticity in both the central nervous system (CNS) and peripheral nervous system (PNS) (Benowitz et al. 1997). While minimally expressed in the PNS, its levels significantly increase following injury (Tetzlaff et al. 1989). Expression of GAP43 was also observed in aganglionic colon sections in Hirschsprung disease, indicating that it is expressed by various types of neurons in the colon (Grynspan et al. 2012).

It is also noteworthy that VIP and/or GAP43 neuronal markers have been included in several previous IBS human and animal model studies, showing upregulation in IBS compared to healthy controls (Dothel et al. 2015; Fujikawa & Tominaga, 2023; Palsson et al., 2004).

4.3 Methods selection and troubleshooting

This study aimed to localize the chosen neuronal markers in the colonic mucosa and visualize their spatial distribution across different available anatomical compartments to better study the effect of neuronal modeling and how nerves have the capacity to behave differently across different anatomical compartments. That is why IHC-staining was the appropriate method of choice for this study.

IHC-staining is a reliable method that detects antigens in cells and tissues with high specificity, through an antigen-antibody interaction mechanism. The signal can be readily visualized under a light microscope and quantified, to give comprehensive results for a marker's abundance and anatomical distribution (Lin & Chen, 2014).

Initially, an IHC-IF method was attempted in order to colocalize the markers, however, the VIP signal using ALEXA Fluor 594 detection chromogen yielded an unreliable punctate signal, possibly due to the fact that, for formalin fixed paraffin embedded (FFPE) tissues, most clinical IF tests are not optimized and can yield autofluorescence (Harms et al., 2023).

Colorimetric colocalization using DAB and Fast Red is widely employed; however, these chromogens are not always optimally suited for simultaneous

application within the same tissue section. In the present study, this limitation may arise because the neuronal markers examined exhibited inverse localization within the same anatomical compartments, such that strong staining for one marker corresponded to relatively weak staining for the other. Under these conditions, overlapping chromogenic signals may not accurately reflect true spatial distribution. Furthermore, as reported by Harms et al. (2023), colocalization of DAB and Fast Red can produce masking effects rather than allowing the two signals to be clearly distinguished, further complicating interpretation.

4.4 Homeostatic architecture in healthy controls

In the healthy controls, there were no correlations observed between mRNA and protein levels for VIP yet GAP43 mRNA expression correlated positively with VIP protein expression across all 4 compartments (Supplementary table S4). Additionally, no correlation of GAP43 protein expression across spatial compartments was observed. However, the VIP protein was tightly coupled across crypt, mucosa, lamina propria, and muscularis mucosa, forming a vertically integrated neurotrophic signal (Supplementary table S1).

This could imply that the enteric neural network in health is homeostatic, spatially coordinated and, with protein localization controlled by circuit-level signalling instead of transcriptional control. In other words, the colonic wall is thus structurally stable, maintaining compartmentalized sensory architecture. These observations set the physiological baseline for identifying disease-underlying mechanistic associations of neuroplasticity, neuronal misdirection, and pain.

This pattern is consistent with a quiescent, structurally stable enteric nervous system in which mature VIPergic innervation is maintained without active neuroplastic remodeling.

4.5 Layer-specific neuronal remodeling in IBS

The most striking feature of the present data is the marked anatomical specificity of neuronal remodeling. GAP43, a marker for axonal growth and synaptic plasticity, was enriched in mucosal compartments and showed a strong association with abdominal pain when measured in the lamina propria. The absence of corresponding correlations with signals from the crypt epithelium compartment, which is not expected to express the GAP43 protein, confirms that the signal is not an artifact of staining, or related to tissue density, but reflects a biologically meaningful neuronal compartment.

The lamina propria is densely populated by immune cells, fibroblasts and vascular structures, and represents a key site of neuroimmune communication in the gut (Chesné et al., 2019). Enteric nerves are therefore known to respond dynamically to inflammatory mediators, cytokines and growth factors (Aguilera-Lizarraga et al, 2022; Chesné et al., 2019) and show sprouting and outgrowth in response to tissue stress (Dothel et al., 2015).

The inverse correlation between GAP43 immunoreactivity in lamina propria and mucosa compartments and abdominal pain severity suggests that mucosal nerve fiber growth in IBS may reflect a compensatory or adaptive response rather than a direct nociception cause. Rather than amplifying pain, increased lamina propria innervation may serve as a stabilizer of mucosal function, modulate immune signals, or dampen inflammatory input to sensory afferents.

This is especially true in the DGBI overlap subgroup, characterized by higher pain burden compared to isolated IBS, where abdominal pain inversely correlated with all layers of GAP43 protein expression.

According to a study by Brown et al., 2016, loss of enteric glia during induced neuroinflammation drive enteric neuron death, which could imply that neuroinflammation in the gut wall can cause loss of nerve fibre outgrowth and consequent neuroimmune dysregulation.

This interpretation is also consistent with preclinical data showing that certain classes of enteric neurons exert anti-inflammatory and protective effects in the gut (Chesné et al., 2019). Thus, the presence of positive neuronal outgrowth and regeneration signal evident by GAP43 immunoreactivity in the lamina propria of IBS cases may be an ongoing attempt of the nervous system to restore homeostasis in a chronically disturbed mucosal environment.

In contrast, the muscularis mucosa showed a very different pattern of remodeling. Here, GAP43 protein levels correlated strongly with GAP43 mRNA expression, indicating that this compartment reflects neuronal cell body density rather than local axonal sprouting, evident by the sporadic identification of relatively large aggregates of cells showing strong GAP43 immunopositivity in exceptionally deep sections that include some submucosa, as shown in Figure 11. This is consistent with the anatomy of the ENS, where neuronal somata are located in the Meissner's plexus in the submucosa (Uesaka et al., 2016).

The muscularis mucosae compartment also showed GAP43 protein coupling with VIP mRNA expression, which means when VIP signalling is transcriptionally upregulated, nerve growth is being directed into the neuromuscular layer. Since VIP is known to promote neuronal survival, promote neurite outgrowth and show a tendency of growth toward smooth muscle and myenteric plexus regions (Brenneman et al. 1985; Iwasaki et al. 2001; Wu et al. 2015), VIP mRNA may be acting as a neurotrophic signal.

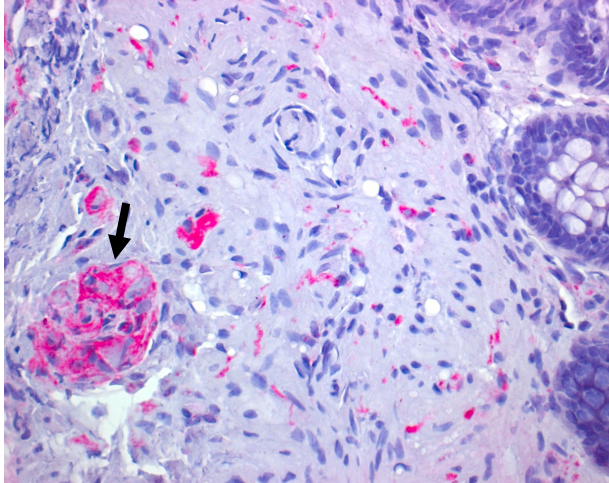


Figure 11. Muscularis mucosa (magnification 40x) of a sample from a participant with IBS, stained for GAP43 (red chromogen). The arrow is pointing at a large aggregate of positive immunoreactive cells only shown in the submucosa where the Meissner's plexus is located.

Bulk transcriptomic data, derived from whole mucosal samples, are therefore likely capturing changes in neuronal density in the muscularis mucosae, rather than fiber density in superficial layers (*Table 2; Table 3*). This explains why mRNA-protein coupling was observed only in this compartment and not in mucosal regions.

4.5.1 Tendency towards regulatory imbalance in DGBI subgroups

VIP immunoreactivity showed a very different distribution and clinical association compared to GAP43. VIP transcription–protein dissociation is shown to be specific to DGBI overlap. VIP mRNA was inversely correlated with VIP protein in the lamina propria exclusively in the DGBI overlap subgroup. This relationship was not observed in IBS patients without overlapping gastroduodenal DGBI, nor in healthy controls or when IBS patients were analyzed as a combined group. By contrast, in IBS participants without DGBI overlap, GAP43 lamina sprouting inversely correlated with localization of VIP protein in crypt adjacent mucosa and lamina propria.

This indicates that in IBS without gastroduodenal DGBI overlap, VIP increase in the muscularis mucosa may drive pain and hypersensitivity symptoms, while GAP43 could be actively sprouting as a compensatory mechanism in the sensitive mucosa. This compensatory pain reducing mechanism related to the active sprouting of nerves is more evident in the DGBI overlap, VIP transcription becomes uncoupled from VIP protein localization at the lamina propria interface. This dissociation may point towards an underlying DGBI overlap mechanism in which, increased VIP transcription does not translate into enhanced VIPergic innervation of the lamina propria. Instead, VIP may be redirected to deeper layers such as the muscularis mucosa, where it was associated with reduced rectal discomfort thresholds in IBS patients in general and more abdominal pain correlation in DGBI non-overlap patients specifically,

i.e., higher VIP levels were associated with increased visceral sensitivity which is summarized in Figure 12. This finding aligns with a large body of experimental literature (Ohman & Simrén, 2007). Such compartment-specific VIP redistribution provides a mechanistic link between elevated VIP transcription, altered nerve localization, and hypersensitivity.

Conversely, IBS patients without gastroduodenal overlap exhibited a distinct pattern: GAP43 protein in the lamina propria was inversely linked with VIP protein in both the lamina propria and mucosa. This indicates that within this subgroup, VIP abundance and neuronal plasticity demonstrate contrasting effects at the mucosal level. This result aligns more closely with a limited compensatory-trial mechanism than with a generalized imbalance between neuroplasticity and neuroimmune remodeling.

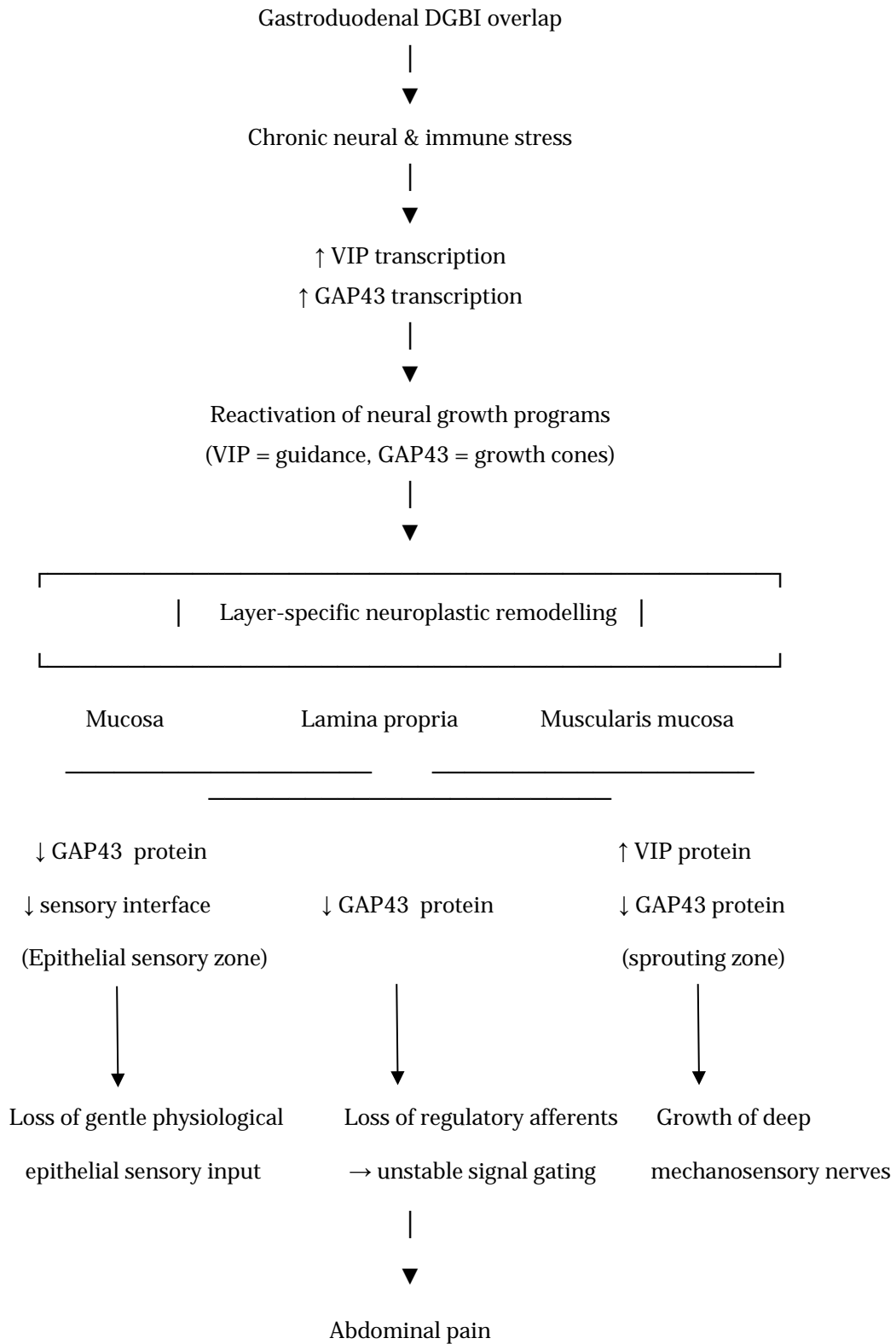


Figure 12 A summary of neuronal remodelling across colonic mucosal anatomical compartments and its symptomatic consequences in IBS with DGBI overlap

5 Ethical aspects and research impact

5.1 Ethical aspects

This study was conducted using human rectal mucosal biopsies and associated clinical and molecular data. As such, it involves human participants and required careful attention to ethical principles including autonomy, confidentiality, non-maleficence, and scientific integrity.

All patients provided informed consent, and the study was approved by the Ethics Review Board in Gothenburg (988-14). Participant clinical data, gene expression data, and immunohistochemical measurements were handled in anonymized form. No personal identifiers were included in the analytical dataset. This ensured compliance with data protection standards.

This study avoided false discovery and overinterpretation by using pre-specified hypotheses (VIP, GAP43 and DGBI subgroups), clearly defining anatomical compartments, and interpreting results based on effect sizes and biological coherence rather than indiscriminate multiple testing. This approach reduces the risk of generating misleading or non-reproducible data claims, which can waste patient trust and research resources.

5.2 Research impact

The study results suggest that IBS shows different neuronal remodeling patterns across the DGBI subgroups. Patients without gastroduodenal DGBI overlap may exhibit compensatory activation of mucosal nerve sprouting pathways, while those with gastroduodenal DGBI overlap may be showing loss of the compensatory mechanism and misdirection of neuronal growth. This theory is supported by increased abdominal pain scores in participants with reduced nerve sprouting, as indicated by low expression of GAP43.

The identification of VIP and GAP43 neuronal remodelling capacity could guide possible therapeutic interventions by targeting how nerves are organized within the gut wall, rather than only suppressing symptoms. Such an approach may be more efficient.

Moreover, GAP43 and VIP show candidacy as biomarkers, within anatomical layer distribution, to diagnose and grade IBS severity.

Methodologically, this study demonstrates the value of integrating compartment-specific protein localization with gene expression and clinical phenotyping, providing a framework for future mechanistic studies of gut–brain disorders.

6 Strengths, limitations and future perspectives

A major strength of this study is the rigorous, blinded, compartment specific quantification of the neuronal markers across a well characterized human cohort. The use of crypt epithelium as internal negative control further validates the specificity of the measurements.

Limitations include the small sample size and the cross-sectional design, which makes it difficult to definitively conclude a cause-and-effect relationship between variables. Additionally, only two neuronal markers were examined separately without colocalization. Future studies should add more diverse neuronal markers and colocalize the markers within anatomical compartments.

Moreover, future studies should combine spatial transcriptomics, multiplex immunohistochemistry and, functional assays to further explore these neurobiological subtypes.

7 References

- Agréus, L., Svärdsudd, K., Nyrén, O., & Tibblin, G. (1995). Irritable bowel syndrome and dyspepsia in the general population: overlap and lack of stability over time. *Gastroenterology*, *109*(3), 671–680. [https://doi.org/10.1016/0016-5085\(95\)90373-9](https://doi.org/10.1016/0016-5085(95)90373-9)
- Aguilera-Lizarraga, J., Hussein, H., & Boeckxstaens, G. E. (2022). Immune activation in irritable bowel syndrome: what is the evidence?. *Nature reviews. Immunology*, *22*(11), 674–686. <https://doi.org/10.1038/s41577-022-00700-9>
- Aziz, I., Palsson, O. S., Törnblom, H., Sperber, A. D., Whitehead, W. E., & Simrén, M. (2018). The prevalence and impact of overlapping Rome IV-diagnosed functional gastrointestinal disorders on somatization, quality of life, and healthcare utilization: A cross-sectional general population study in three countries. *American Journal of Gastroenterology*, *113*(1), 86–96. <https://doi.org/10.1038/ajg.2017.421>
- Azpiroz, F., Bouin, M., Camilleri, M., Mayer, E. A., Poitras, P., Serra, J., & Spiller, R. C. (2007). Mechanisms of hypersensitivity in IBS and functional disorders. *Neurogastroenterology and Motility*, *19*(1 Suppl), 62–88. <https://doi.org/10.1111/j.1365-2982.2006.00875.x>
- Banks, M. R., Farthing, M. J., Robberecht, P., & Burleigh, D. E. (2005). Antisecretory actions of a novel vasoactive intestinal polypeptide (VIP) antagonist in human and rat small intestine. *British Journal of Pharmacology*, *144*(7), 994–1001.
- Bankhead, P., Loughrey, M.B., Fernández, J.A. *et al.* QuPath: Open source software for digital pathology image analysis. *Sci Rep* **7**, 16878 (2017). <https://doi.org/10.1038/s41598-017-17204-5>
- Barbara, G., Barbaro, M. R., Cremon, C., Marasco, G., Savarino, E., Guglielmetti, S., ... Collins, S. M. (2024). Molecular mechanisms underlying loss of vascular and epithelial integrity in irritable bowel syndrome. *Gastroenterology*, *167*(6), 1152–1166. <https://doi.org/10.1053/j.gastro.2024.07.004>
- Benowitz, L. I., & Routtenberg, A. (1997). GAP-43: An intrinsic determinant of neuronal development and plasticity. *Trends in Neurosciences*, *20*(2), 84–91.
- Brenneman, D. E., Eiden, L. E., & Siegel, R. E. (1985). Neurotrophic action of VIP on spinal cord cultures. *Peptides*, *6*(Suppl 2), 35–39.
- Brown, I. A., McClain, J. L., Watson, R. E., Patel, B. A., & Gulbransen, B. D. (2016). Enteric glia mediate neuron death in colitis through purinergic pathways that require connexin-43 and nitric oxide. *Cellular and molecular gastroenterology and hepatology*, *2*(1), 77–91. <https://doi.org/10.1016/j.jcmgh.2015.08.007>

Bureychak, T., Faresjö, Å., Sjö Dahl, J., Norlin, A. K., & Walter, S. (2022). Symptoms and health experience in irritable bowel syndrome with focus on men. *Neurogastroenterology and motility*, *34*(11), e14430. <https://doi.org/10.1111/nmo.14430>

Camilleri, M., Carlson, P., Acosta, A., Busciglio, I., Nair, A. A., Gibbons, S. J., Farrugia, G., & Klee, E. W. (2014). RNA sequencing shows transcriptomic changes in rectosigmoid mucosa in patients with irritable bowel syndrome-diarrhea: A pilot case-control study. *American Journal of Physiology-Gastrointestinal and Liver Physiology*, *306*(12), G1089–G1098.

Chesné, J., Cardoso, V., & Veiga-Fernandes, H. (2019). Neuro-immune regulation of mucosal physiology. *Mucosal immunology*, *12*(1), 10–20. <https://doi.org/10.1038/s41385-018-0063-y>

Dothel, G., Barbaro, M. R., Boudin, H., Vasina, V., Cremon, C., Gargano, L., Bellacosa, L., De Giorgio, R., Le Berre-Scoul, C., Aubert, P., Neunlist, M., De Ponti, F., Stanghellini, V., & Barbara, G. (2015). Nerve fiber outgrowth is increased in the intestinal mucosa of patients with irritable bowel syndrome. *Gastroenterology*, *148*(5), 1002–1011.e4. <https://doi.org/10.1053/j.gastro.2015.01.042>

Drossman, D. A. (2016). In D. A. Drossman, L. C. Chang, W. J. Kellow, J. Tack, & W. E. Whitehead (Eds.), *Rome IV functional gastrointestinal disorders: Disorders of gut-brain interaction* (pp. 549–576). The Rome Foundation.

Frankish, A., Carbonell-Sala, S., Diekhans, M., Jungreis, I., Loveland, J. E., Mudge, J. M., Sisu, C., Wright, J. C., Arnan, C., Barnes, I., Banerjee, A., Bennett, R., Berry, A., Bignell, A., Boix, C., Calvet, F., Cerdán-Vélez, D., Cunningham, F., Davidson, C., Donaldson, S., ... Flicek, P. (2023). GENCODE: reference annotation for the human and mouse genomes in 2023. *Nucleic acids research*, *51*(D1), D942–D949. <https://doi.org/10.1093/nar/gkac1071>

Fujikawa, Y., & Tominaga, K. (2023). Enhanced neuron-glia network in the submucosa and increased neuron outgrowth into the mucosa are associated with distinctive expressions of neuronal factors in the colon of rat IBS model. *Neurogastroenterology and Motility*, *35*(9), e14595.

Galligan, J. J., Furness, J. B., & Costa, M. (1989). Migration of the myoelectric complex after interruption of the myenteric plexus: Intestinal transection and regeneration of enteric nerves in the guinea pig. *Gastroenterology*, *97*(5), 1135–1146.

Grynspan, D., Giassi, A. C., Cadonic, R., Bettolli, M., Schock, S. C., Perozzo, A., & Staines, W. A. (2012). Growth-associated protein-43 (GAP-43) expression in ganglionic and aganglionic colon. *Pediatric and Developmental Pathology*, *15*(5), 360–368. <https://doi.org/10.2350/11-10-1106-OA.1>

Harms, P. W., Frankel, T. L., Moutafi, M., Rao, A., Rimm, D. L., Taube, J. M., Thomas, D., Chan, M. P., & Pantanowitz, L. (2023). Multiplex Immunohistochemistry and Immunofluorescence: A Practical Update for Pathologists. *Modern pathology : an official journal of the United States and Canadian Academy of Pathology, Inc*, *36*(7), 100197. <https://doi.org/10.1016/j.modpat.2023.100197>

He, Q., Dent, E. W., & Meiri, K. F. (1997). Modulation of actin filament behavior by GAP-43 (neuromodulin) is dependent on the phosphorylation status of serine 41. *The Journal of Neuroscience*, *17*(10), 3515–3524. <https://doi.org/10.1523/JNEUROSCI.17-10-03515.1997>

Iwasaki, Y., Ikeda, K., Ichikawa, Y., & Igarashi, O. (2001). Vasoactive intestinal peptide influences neurite outgrowth in cultured rat spinal cord neurons. *Neurological Research*, *23*(8), 851–854. <https://doi.org/10.1179/016164101101199117>

Kaji, M., Fujiwara, Y., Shiba, M., Kohata, Y., Yamagami, H., Tanigawa, T., Watanabe, K., Watanabe, T., Tominaga, K., & Arakawa, T. (2010). Prevalence of overlaps between GERD, FD and IBS and impact on health-related quality of life. *Journal of gastroenterology and hepatology*, *25*(6), 1151–1156. <https://doi.org/10.1111/j.1440-1746.2010.06249.x>

Lee, H. J., Lee, S. Y., Kim, J. H., Sung, I. K., Park, H. S., Jin, C. J., Kang, S. G., Yoon, H., & Chun, H. J. (2010). Depressive mood and quality of life in functional gastrointestinal disorders: differences between functional dyspepsia, irritable bowel syndrome and overlap syndrome. *General hospital psychiatry*, *32*(5), 499–502. <https://doi.org/10.1016/j.genhosppsy.2010.05.002>

Lin, F., & Chen, Z. (2014). Standardization of diagnostic immunohistochemistry: literature review and geisinger experience. *Archives of pathology & laboratory medicine*, *138*(12), 1564–1577. <https://doi.org/10.5858/arpa.2014-0074-RA>

Mearin, F., Lacy, B. E., Chang, L., Chey, W. D., Lembo, A. J., Simren, M., & Spiller, R. (2016). Bowel disorders. *Gastroenterology*, *150*(6), 1393–1407.e5. <https://doi.org/10.1053/j.gastro.2016.02.031>

Mertz, H., Naliboff, B., Munakata, J., Niazi, N., & Mayer, E. A. (1995). Altered rectal perception is a biological marker of patients with irritable bowel syndrome. *Gastroenterology*, *109*(1), 40–52. [https://doi.org/10.1016/0016-5085\(95\)90269-8](https://doi.org/10.1016/0016-5085(95)90269-8)

Love, M. I., Huber, W., & Anders, S. (2014). Moderated estimation of fold change and dispersion for RNA-seq data with DESeq2. *Genome biology*, *15*(12), 550. <https://doi.org/10.1186/s13059-014-0550-8>

Lovell, R. M., & Ford, A. C. (2012). Effect of gender on prevalence of irritable bowel syndrome in the community: systematic review and meta-analysis. *The American journal of gastroenterology*, *107*(7), 991–1000. <https://doi.org/10.1038/ajg.2012.131>

Ohman, L., & Simrén, M. (2007). New insights into the pathogenesis and pathophysiology of irritable bowel syndrome. *Digestive and liver disease : official journal of the Italian Society of Gastroenterology and the Italian Association for the Study of the Liver*, *39*(3), 201–215. <https://doi.org/10.1016/j.dld.2006.10.014>

Oka, P., Parr, H., Barberio, B., Black, C. J., Savarino, E. V., & Ford, A. C. (2020). Global prevalence of irritable bowel syndrome according to Rome III or IV criteria: A systematic review and meta-analysis. *The Lancet Gastroenterology & Hepatology*, *5*(10), 908–917. [https://doi.org/10.1016/S2468-1253\(20\)30217-X](https://doi.org/10.1016/S2468-1253(20)30217-X)

Palsson, O. S., Morteau, O., Bozyski, E. M., Woosley, J. T., Sartor, R. B., Davies, M. J., Johnson, D. A., Turner, M. J., & Whitehead, W. E. (2004). Elevated vasoactive intestinal peptide concentrations in patients with irritable bowel syndrome. *Digestive Diseases and Sciences*, *49*(7–8), 1236–1243. <https://doi.org/10.1023/B:DDAS.0000034552.40589.55>

Schmulson, M. J., & Drossman, D. A. (2017). What is new in Rome IV. *Journal of Neurogastroenterology and Motility*, *23*(2), 151–163. <https://doi.org/10.5056/jnm16214>

Simrén, M., Törnblom, H., Palsson, O. S., van Tilburg, M. A. L., Van Oudenhove, L., Tack, J., & Whitehead, W. E. (2018). Visceral hypersensitivity is associated with GI symptom severity in functional GI disorders: consistent findings from five different patient cohorts. *Gut*, *67*(2), 255–262. <https://doi.org/10.1136/gutjnl-2016-312361>

Soneson, C., Love, M. I., & Robinson, M. D. (2015). Differential analyses for RNA-seq: transcript-level estimates improve gene-level inferences. *F1000Research*, *4*, 1521. <https://doi.org/10.12688/f1000research.7563.2>

Sperber, A. D., & Drossman, D. A. (2011). Review article: The functional abdominal pain syndrome. *Alimentary Pharmacology & Therapeutics*, *33*(5), 514–524. <https://doi.org/10.1111/j.1365-2036.2010.04537.x>

Sperber, A. D., Bangdiwala, S. I., Drossman, D. A., Ghoshal, U. C., Simren, M., Tack, J., Whitehead, W. E., Dumitrascu, D. L., Fang, X., Fukudo, S., Kellow, J., Okeke, E., Quigley, E. M. M., Schmulson, M., Whorwell, P., Archanpong, T., Adibi, P., ... Palsson, O. S. (2021). Worldwide prevalence and burden of functional gastrointestinal disorders: Results of the Rome Foundation Global Study. *Gastroenterology*, *160*(1), 99–114.e3. <https://doi.org/10.1053/j.gastro.2020.04.014>

Sperber, A. D., Freud, T., Aziz, I., Palsson, O. S., Drossman, D. A., Dumitrascu, D. L., Fang, X., Fukudo, S., Ghoshal, U. C., Kellow, J., Khatun, R., Okeke, E., Quigley, E. M. M., Schmulson, M., Simren, M., Tack, J., Whitehead, W. E., Whorwell, P., & Bangdiwala, S. I. (2022). Greater overlap of Rome IV disorders of gut-brain interactions leads to increased disease severity and poorer quality of life. *Clinical Gastroenterology*

and *Hepatology*, 20(5), e945–e956.
<https://doi.org/10.1016/j.cgh.2020.09.030>

Suzuki, H., & Hibi, T. (2011). Overlap syndrome of functional dyspepsia and irritable bowel syndrome - are both diseases mutually exclusive?. *Journal of neurogastroenterology and motility*, 17(4), 360–365.
<https://doi.org/10.5056/jnm.2011.17.4.360>

Svedlund, J., Sjödin, I., & Dotevall, G. (1988). GSRS--a clinical rating scale for gastrointestinal symptoms in patients with irritable bowel syndrome and peptic ulcer disease. *Digestive diseases and sciences*, 33(2), 129–134.
<https://doi.org/10.1007/BF01535722>

Tack, J., Caenepeel, P., Fischler, B., Piessevaux, H., & Janssens, J. (2001). Symptoms associated with hypersensitivity to gastric distention in functional dyspepsia. *Gastroenterology*, 121(3), 526–535.
<https://doi.org/10.1053/gast.2001.27180>

Tack, J., Talley, N. J., Camilleri, M., Holtmann, G., Hu, P., Malagelada, J. R., & Stanghellini, V. (2006). Functional gastroduodenal disorders. *Gastroenterology*, 130(5), 1466–1479.
<https://doi.org/10.1053/j.gastro.2005.11.059>

Talley, N. J., Zinsmeister, A. R., Schleck, C. D., & Melton, L. J., 3rd (1992). Dyspepsia and dyspepsia subgroups: a population-based study. *Gastroenterology*, 102(4 Pt 1), 1259–1268.

Tetzlaff, W., Zwiers, H., Lederis, K., Cassar, L., & Bisby, M. A. (1989). Axonal transport and localization of B-50/GAP-43-like immunoreactivity in regenerating sciatic and facial nerves of the rat. *The Journal of Neuroscience*, 9(4), 1303–1313.
<https://doi.org/10.1523/JNEUROSCI.09-04-01303.1989>

Uesaka, T., Young, H. M., Pachnis, V., & Enomoto, H. (2016). Development of the intrinsic and extrinsic innervation of the gut. *Developmental biology*, 417(2), 158–167. <https://doi.org/10.1016/j.ydbio.2016.04.016>

Van den Houte, K., Carbone, F., Goelen, N., Schol, J., Masuy, I., Arts, J., Caenepeel, P., Staessen, D., Vergauwe, P., Van Roey, G., Latour, P., Piessevaux, H., Maldague, P., Gerkens, A., Wuestenberghs, F., Vandenberghe, A., & Tack, J. (2021).

Effects of Rome IV definitions of functional dyspepsia subgroups in secondary care. *Clinical Gastroenterology and Hepatology*, 19(8), 1620–1626.
<https://doi.org/10.1016/j.cgh.2020.04.056>

Wang, A., Liao, X., Xiong, L., Peng, S., Xiao, Y., Liu, S., Hu, P., & Chen, M. (2008). The clinical overlap between functional dyspepsia and irritable bowel syndrome based on Rome III criteria. *BMC gastroenterology*, 8, 43.
<https://doi.org/10.1186/1471-230X-8-43>

Whitehead, W. E., Holtkotter, B., Enck, P., Hoelzl, R., Holmes, K. D., Anthony, J., Shabsin, H. S., & Schuster, M. M. (1990). Tolerance for rectosigmoid distention in irritable bowel syndrome. *Gastroenterology*, *98*(5 Pt 1), 1187–1192. [https://doi.org/10.1016/0016-5085\(90\)90332-u](https://doi.org/10.1016/0016-5085(90)90332-u)

Wu, X., Conlin, V. S., Morampudi, V., Ryz, N. R., Nasser, Y., Bhinder, G., ... Khan, W. I. (2015). Vasoactive intestinal polypeptide promotes intestinal barrier homeostasis and protection against colitis in mice. *PLoS ONE*, *10*(5), e0125225. <https://doi.org/10.1371/journal.pone.0125225>

Zigmond, A. S., & Snaith, R. P. (1983). The hospital anxiety and depression scale. *Acta psychiatrica Scandinavica*, *67*(6), 361–370. <https://doi.org/10.1111/j.1600-0447.1983.tb09716.x>

Supplementary information

Supplementary Table S1. Pairwise correlations of protein expression across anatomical compartments for each marker in IBS patients and HC. Pairwise correlations of protein expression levels between anatomical compartments within the same marker. For each marker, protein expression was correlated between two different anatomical compartments (four compartments total), generating compartment-to-compartment comparisons. Correlation coefficients (r) and corresponding p -values are shown.

Marker	Layer1	Layer2	r	p	Sub-group
GAP43	Crypt	Lamina propria	0.54	0.002	IBS
GAP43	Crypt	Mucosa	0.79	<0.001	IBS
GAP43	Crypt	Muscularis mucosae	0.55	0.002	IBS
GAP43	Lamina propria	Mucosa	0.81	<0.001	IBS
GAP43	Lamina propria	Muscularis mucosae	0.62	<0.001	IBS
GAP43	Mucosa	Muscularis mucosa	0.56	0.002	IBS
VIP	Crypt	Lamina propria	0.59	<0.001	IBS
VIP	Crypt	Mucosa	0.79	<0.001	IBS
VIP	Crypt	Muscularis mucosae	0.65	<0.001	IBS
VIP	Lamina propria	Mucosa	0.94	<0.001	IBS
VIP	Lamina propria	Muscularis mucosae	0.42	0.019	IBS
VIP	Mucosa	Muscularis mucosae	0.59	<0.001	IBS
GAP43	Crypt	Lamina propria	0.095	0.84	HC
GAP43	Crypt	Mucosa	0.69	0.069	HC
GAP43	Crypt	Muscularis mucosae	-0.086	0.92	HC
GAP43	Lamina propria	Mucosa	0.48	0.24	HC
GAP43	Lamina propria	Muscularis mucosae	0.42	0.42	HC
GAP43	Mucosa	Muscularis mucosae	0.029	1	HC
VIP	Crypt	Lamina propria	0.83	0.015	HC
VIP	Crypt	Mucosa	0.85	0.007	HC
VIP	Crypt	Muscularis mucosae	0.821	0.034	HC
VIP	Lamina propria	Mucosa	0.97	<0.001	HC

Marker	Layer1	Layer2	r	p	Sub-group
VIP	Lamina propria	Muscularis mucosae	0.75	0.066	HC
VIP	Mucosa	Muscularis mucosae	0.72	0.068	HC

Supplementary Table S2 Correlations between protein expression across the 4 compartments and clinical outcome within DGBI overlap subgroup

DGBI_group	Marker	Layer	Symptom	r	p
IBS_DGBI	GAP43	Crypt	Abdominal_pain	-0.35	0.190
IBS_DGBI	GAP43	Crypt	Baro_discomfort_ml	-0.15	0.580
IBS_DGBI	GAP43	Crypt	Baro_firstsens_ml	0.08	0.760
IBS_DGBI	GAP43	Crypt	HAD_anxiety	0.33	0.210
IBS_DGBI	GAP43	Crypt	HAD_depression	0.36	0.170
IBS_DGBI	GAP43	Lamina_properia	Abdominal_pain	-0.58	0.020
IBS_DGBI	GAP43	Lamina_properia	Baro_discomfort_ml	-0.11	0.680
IBS_DGBI	GAP43	Lamina_properia	Baro_firstsens_ml	0.12	0.670
IBS_DGBI	GAP43	Lamina_properia	HAD_anxiety	0.22	0.410
IBS_DGBI	GAP43	Lamina_properia	HAD_depression	0.18	0.500
IBS_DGBI	GAP43	Mucosa	Abdominal_pain	-0.49	0.054
IBS_DGBI	GAP43	Mucosa	Baro_discomfort_ml	-0.14	0.600
IBS_DGBI	GAP43	Mucosa	Baro_firstsens_ml	0.05	0.850
IBS_DGBI	GAP43	Mucosa	HAD_anxiety	0.27	0.310
IBS_DGBI	GAP43	Mucosa	HAD_depression	0.29	0.270
IBS_DGBI	GAP43	Muscularis_mucosa	Abdominal_pain	-0.47	0.076
IBS_DGBI	GAP43	Muscularis_mucosa	Baro_discomfort_ml	-0.11	0.700
IBS_DGBI	GAP43	Muscularis_mucosa	Baro_firstsens_ml	-0.01	0.990
IBS_DGBI	GAP43	Muscularis_mucosa	HAD_anxiety	0.38	0.170
IBS_DGBI	GAP43	Muscularis_mucosa	HAD_depression	0.40	0.140
IBS_DGBI	VIP	Crypt	Abdominal_pain	0.28	0.290
IBS_DGBI	VIP	Crypt	Baro_discomfort_ml	-0.26	0.340
IBS_DGBI	VIP	Crypt	Baro_firstsens_ml	0.17	0.520
IBS_DGBI	VIP	Crypt	HAD_anxiety	-0.24	0.370
IBS_DGBI	VIP	Crypt	HAD_depression	-0.20	0.470
IBS_DGBI	VIP	Lamina_properia	Abdominal_pain	0.22	0.410
IBS_DGBI	VIP	Lamina_properia	Baro_discomfort_ml	-0.18	0.510
IBS_DGBI	VIP	Lamina_properia	Baro_firstsens_ml	0.21	0.440
IBS_DGBI	VIP	Lamina_properia	HAD_anxiety	-0.16	0.550
IBS_DGBI	VIP	Lamina_properia	HAD_depression	0.11	0.680
IBS_DGBI	VIP	Mucosa	Abdominal_pain	0.28	0.290
IBS_DGBI	VIP	Mucosa	Baro_discomfort_ml	-0.19	0.480
IBS_DGBI	VIP	Mucosa	Baro_firstsens_ml	0.18	0.490
IBS_DGBI	VIP	Mucosa	HAD_anxiety	-0.20	0.470
IBS_DGBI	VIP	Mucosa	HAD_depression	0.00	0.990
IBS_DGBI	VIP	Muscularis_mucosa	Abdominal_pain	0.22	0.420
IBS_DGBI	VIP	Muscularis_mucosa	Baro_discomfort_ml	-0.29	0.280
IBS_DGBI	VIP	Muscularis_mucosa	Baro_firstsens_ml	-0.05	0.850
IBS_DGBI	VIP	Muscularis_mucosa	HAD_anxiety	0.19	0.480
IBS_DGBI	VIP	Muscularis_mucosa	HAD_depression	0.19	0.470

Supplementary Table S3 Correlations between protein expression across the 4 compartments and clinical outcome within DGBI non overlap (IBS noDGBI) subgroup

DGBI_group	Marker	Layer	Symptom	r	p
IBS_noDGBI	GAP43	Crypt	Abdominal_pain	-0.07	0.790
IBS_noDGBI	GAP43	Crypt	Baro_discomfort_ml	-0.34	0.190
IBS_noDGBI	GAP43	Crypt	Baro_firstsens_ml	-0.18	0.500
IBS_noDGBI	GAP43	Crypt	HAD_anxiety	-0.19	0.490
IBS_noDGBI	GAP43	Crypt	HAD_depression	-0.18	0.520
IBS_noDGBI	GAP43	Lamina_properia	Abdominal_pain	-0.32	0.220
IBS_noDGBI	GAP43	Lamina_properia	Baro_discomfort_ml	-0.17	0.530
IBS_noDGBI	GAP43	Lamina_properia	Baro_firstsens_ml	-0.11	0.690
IBS_noDGBI	GAP43	Lamina_properia	HAD_anxiety	-0.12	0.670
IBS_noDGBI	GAP43	Lamina_properia	HAD_depression	-0.36	0.180
IBS_noDGBI	GAP43	Mucosa	Abdominal_pain	-0.24	0.360
IBS_noDGBI	GAP43	Mucosa	Baro_discomfort_ml	-0.18	0.520
IBS_noDGBI	GAP43	Mucosa	Baro_firstsens_ml	-0.13	0.630
IBS_noDGBI	GAP43	Mucosa	HAD_anxiety	-0.14	0.610
IBS_noDGBI	GAP43	Mucosa	HAD_depression	-0.37	0.170
IBS_noDGBI	GAP43	Muscularis_mucosa	Abdominal_pain	-0.25	0.370
IBS_noDGBI	GAP43	Muscularis_mucosa	Baro_discomfort_ml	0.22	0.430
IBS_noDGBI	GAP43	Muscularis_mucosa	Baro_firstsens_ml	0.22	0.420
IBS_noDGBI	GAP43	Muscularis_mucosa	HAD_anxiety	-0.01	0.980
IBS_noDGBI	GAP43	Muscularis_mucosa	HAD_depression	-0.32	0.260
IBS_noDGBI	VIP	Crypt	Abdominal_pain	0.28	0.290
IBS_noDGBI	VIP	Crypt	Baro_discomfort_ml	-0.28	0.290
IBS_noDGBI	VIP	Crypt	Baro_firstsens_ml	-0.11	0.680
IBS_noDGBI	VIP	Crypt	HAD_anxiety	-0.10	0.720
IBS_noDGBI	VIP	Crypt	HAD_depression	0.21	0.460
IBS_noDGBI	VIP	Lamina_properia	Abdominal_pain	0.16	0.560
IBS_noDGBI	VIP	Lamina_properia	Baro_discomfort_ml	-0.15	0.580
IBS_noDGBI	VIP	Lamina_properia	Baro_firstsens_ml	-0.15	0.590
IBS_noDGBI	VIP	Lamina_properia	HAD_anxiety	-0.14	0.610
IBS_noDGBI	VIP	Lamina_properia	HAD_depression	0.09	0.750
IBS_noDGBI	VIP	Mucosa	Abdominal_pain	0.30	0.250
IBS_noDGBI	VIP	Mucosa	Baro_discomfort_ml	-0.24	0.370
IBS_noDGBI	VIP	Mucosa	Baro_firstsens_ml	-0.20	0.450
IBS_noDGBI	VIP	Mucosa	HAD_anxiety	-0.06	0.820
IBS_noDGBI	VIP	Mucosa	HAD_depression	0.20	0.470
IBS_noDGBI	VIP	Muscularis_mucosa	Abdominal_pain	0.59	0.022
IBS_noDGBI	VIP	Muscularis_mucosa	Baro_discomfort_ml	-0.38	0.170
IBS_noDGBI	VIP	Muscularis_mucosa	Baro_firstsens_ml	-0.10	0.720
IBS_noDGBI	VIP	Muscularis_mucosa	HAD_anxiety	0.05	0.870
IBS_noDGBI	VIP	Muscularis_mucosa	HAD_depression	-0.13	0.660

Supplementary Table S4 correlations between VIP and GAP43 mRNA transcription and their protein expression OD across all 4 compartments in HC. Pairwise correlations of protein expression levels between anatomical compartments and marker mRNA expression. Correlation coefficients (Spearman_rho) and corresponding p-values are shown.

Marker	Layer	Spearman_rho	p_value
VIP	GAP43_mucosa	0.4047619	0.326835317
VIP	GAP43_muscularis_mucosa	-0.2571429	0.658333333
VIP	GAP43_Crypt	-0.2619048	0.536408730
VIP	GAP43_Lamina_properia	0.5476190	0.170982143
VIP	VIP_mucosa	0.3712641	0.365202058
VIP	VIP_muscularis_mucosa	0.4285714	0.353571429
VIP	VIP_Crypt	0.6904762	0.069394841
VIP	VIP_Lamina_properia	0.3095238	0.461805556
GAP43	GAP43_mucosa	0.0952381	0.840128968
GAP43	GAP43_muscularis_mucosa	-0.3714286	0.497222222
GAP43	GAP43_Crypt	-0.2380952	0.582142857
GAP43	GAP43_Lamina_properia	0.4047619	0.326835317
GAP43	VIP_mucosa	0.7185758	0.044622610
GAP43	VIP_muscularis_mucosa	0.8571429	0.023809524
GAP43	VIP_Crypt	0.9523810	0.001140873
GAP43	VIP_Lamina_properia	0.7142857	0.057589286

Supplementary table S5 correlations between VIP and GAP43 mRNA transcription and their protein expression OD across all 4 compartments in IBS non-overlap subgroup. Pairwise correlations of protein expression levels between anatomical compartments and marker mRNA expression. Correlation coefficients (Spearman_rho) and corresponding p-values are shown.

Marker	Layer	Spearman_rho	p_value
VIP	GAP43_mucosa	-0.02941176	0.91709386
VIP	GAP43_muscularis_mucosa	0.45000000	0.09435196
VIP	GAP43_Crypt	0.16176471	0.54860525
VIP	GAP43_Lamina_properia	0.02647059	0.92579618
VIP	VIP_mucosa	-0.11176471	0.68053314
VIP	VIP_muscularis_mucosa	0.14642857	0.60238315
VIP	VIP_Crypt	0.19705882	0.46318549
VIP	VIP_Lamina_properia	-0.10588235	0.69676700
GAP43	GAP43_mucosa	0.15822658	0.55836398
GAP43	GAP43_muscularis_mucosa	0.44866686	0.09344570
GAP43	GAP43_Crypt	0.17016821	0.52864198
GAP43	GAP43_Lamina_properia	0.06269355	0.81758061
GAP43	VIP_mucosa	0.08060599	0.76665549
GAP43	VIP_muscularis_mucosa	-0.08108437	0.77390788
GAP43	VIP_Crypt	0.38213212	0.14411027
GAP43	VIP_Lamina_properia	0.08060599	0.76665549

Supplementary table S6 correlations between VIP and GAP43 mRNA transcription and their protein expression OD across all 4 compartments in IBS DGBI-overlap subgroup. Pairwise correlations of protein expression levels between anatomical compartments and marker mRNA expression. Correlation coefficients (Spearman_rho) and corresponding p-values are shown.

Marker	Layer	Spearman_rho	p_value
VIP	GAP43_mucosa	-0.01764706	0.95194851
VIP	GAP43_muscularis_mucosa	0.13571429	0.62971552
VIP	GAP43_Crypt	0.12058824	0.65643826
VIP	GAP43_Lamina_properia	-0.05000000	0.85648749
VIP	VIP_mucosa	-0.38410606	0.14187692
VIP	VIP_muscularis_mucosa	0.06470588	0.81365136
VIP	VIP_Crypt	-0.20588235	0.44295912
VIP	VIP_Lamina_properia	-0.51764706	0.04232162
GAP43	GAP43_mucosa	-0.10000000	0.71313005
GAP43	GAP43_muscularis_mucosa	0.16428571	0.55796050
GAP43	GAP43_Crypt	0.15882353	0.55603227
GAP43	GAP43_Lamina_properia	0.01470588	0.96067788
GAP43	VIP_mucosa	-0.16777046	0.53455186
GAP43	VIP_muscularis_mucosa	-0.11470588	0.67246662
GAP43	VIP_Crypt	0.02352941	0.93450670
GAP43	VIP_Lamina_properia	-0.37941176	0.14798277

Supplementary Table S7. Correlations between VIP and GAP43 protein expression across anatomical compartments within combined IBS cohort. For each anatomical compartment, protein expression levels of VIP were correlated with GAP43, generating compartment-specific VIP–GAP43 comparisons across four compartments. Correlation coefficients (Spearman_rho) and corresponding p-values are shown.

Group	VIP_Layer	GAP43_Layer	Spearman_rho	p_value
IBS	VIP_mucosa	GAP43_mucosa	-0.28762604	0.110429697
IBS	VIP_mucosa	GAP43_muscularis_mucosa	-0.32265243	0.082034735
IBS	VIP_mucosa	GAP43_Crypt	-0.21741522	0.231963077
IBS	VIP_mucosa	GAP43_Lamina_properia	-0.35472045	0.046362368
IBS	VIP_muscularis_mucosa	GAP43_mucosa	-0.01008065	0.957077437
IBS	VIP_muscularis_mucosa	GAP43_muscularis_mucosa	-0.12836485	0.499032221
IBS	VIP_muscularis_mucosa	GAP43_Crypt	0.12338710	0.508424374
IBS	VIP_muscularis_mucosa	GAP43_Lamina_properia	-0.18104839	0.329710702
IBS	VIP_Crypt	GAP43_mucosa	-0.23203812	0.201281632
IBS	VIP_Crypt	GAP43_muscularis_mucosa	-0.21290323	0.258653609
IBS	VIP_Crypt	GAP43_Crypt	-0.04105572	0.823457712
IBS	VIP_Crypt	GAP43_Lamina_properia	-0.25183284	0.164397943
IBS	VIP_Lamina_properia	GAP43_mucosa	-0.20307918	0.264958001
IBS	VIP_Lamina_properia	GAP43_muscularis_mucosa	-0.30945495	0.096099348
IBS	VIP_Lamina_properia	GAP43_Crypt	-0.22910557	0.207196985
IBS	VIP_Lamina_properia	GAP43_Lamina_properia	-0.31085044	0.083332632

Supplementary Table S8. Correlations between VIP and GAP43 protein expression across anatomical compartments within IBS non-overlap subgroup (GD_DGBI_No). For each anatomical compartment, protein expression levels of VIP were correlated with GAP43, generating compartment-specific VIP–GAP43 comparisons across four compartments. Correlation coefficients (Spearman_rho) and corresponding p-values are shown.

Group	VIP_Layer	GAP43_Layer	Spearman_rho	p_value
GD_DGBI_No	VIP_mucosa	GAP43_mucosa	-0.37941176	0.147227134
GD_DGBI_No	VIP_mucosa	GAP43_muscularis_mucosa	-0.37500000	0.168432750
GD_DGBI_No	VIP_mucosa	GAP43_Crypt	-0.20000000	0.457687905
GD_DGBI_No	VIP_mucosa	GAP43_Lamina_properia	-0.60294118	0.013424125
GD_DGBI_No	VIP_muscularis_mucosa	GAP43_mucosa	-0.04285714	0.879460313
GD_DGBI_No	VIP_muscularis_mucosa	GAP43_muscularis_mucosa	0.11428571	0.685065763
GD_DGBI_No	VIP_muscularis_mucosa	GAP43_Crypt	0.37857143	0.164090827
GD_DGBI_No	VIP_muscularis_mucosa	GAP43_Lamina_properia	-0.18928571	0.499263033
GD_DGBI_No	VIP_Crypt	GAP43_mucosa	-0.20000000	0.457687905
GD_DGBI_No	VIP_Crypt	GAP43_muscularis_mucosa	-0.04642857	0.869491526
GD_DGBI_No	VIP_Crypt	GAP43_Crypt	0.18529412	0.492057050
GD_DGBI_No	VIP_Crypt	GAP43_Lamina_properia	-0.32941176	0.212801426
GD_DGBI_No	VIP_Lamina_properia	GAP43_mucosa	-0.36764706	0.161232358
GD_DGBI_No	VIP_Lamina_properia	GAP43_muscularis_mucosa	-0.40000000	0.139595129
GD_DGBI_No	VIP_Lamina_properia	GAP43_Crypt	-0.33235294	0.208499828
GD_DGBI_No	VIP_Lamina_properia	GAP43_Lamina_properia	-0.64411765	0.007081524

Supplementary Table S9. Correlations between VIP and GAP43 protein expression across anatomical compartments within IBS DGBI-overlap subgroup (GD_DGBI_Yes). For each anatomical compartment, protein expression levels of VIP were correlated with GAP43, generating compartment-specific VIP–GAP43 comparisons across four compartments. Correlation coefficients (Spearman_rho) and corresponding p-values are shown.

Group	VIP_Layer	GAP43_Layer	Spearman_rho	p_value
GD_DGBI_Yes	VIP_mucosa	GAP43_mucosa	-0.19278887	0.474389415
GD_DGBI_Yes	VIP_mucosa	GAP43_muscularis_mucosa	-0.28775704	0.298340072
GD_DGBI_Yes	VIP_mucosa	GAP43_Crypt	-0.15599710	0.563991671
GD_DGBI_Yes	VIP_mucosa	GAP43_Lamina_properia	-0.11773366	0.664107501
GD_DGBI_Yes	VIP_muscularis_mucosa	GAP43_mucosa	-0.03823529	0.888197654
GD_DGBI_Yes	VIP_muscularis_mucosa	GAP43_muscularis_mucosa	-0.38928571	0.151511937
GD_DGBI_Yes	VIP_muscularis_mucosa	GAP43_Crypt	-0.03823529	0.888197654
GD_DGBI_Yes	VIP_muscularis_mucosa	GAP43_Lamina_properia	-0.23235294	0.386511350
GD_DGBI_Yes	VIP_Crypt	GAP43_mucosa	-0.23823529	0.374254130
GD_DGBI_Yes	VIP_Crypt	GAP43_muscularis_mucosa	-0.32857143	0.231809697
GD_DGBI_Yes	VIP_Crypt	GAP43_Crypt	-0.14705882	0.586793394
GD_DGBI_Yes	VIP_Crypt	GAP43_Lamina_properia	-0.19705882	0.464464211
GD_DGBI_Yes	VIP_Lamina_properia	GAP43_mucosa	-0.10000000	0.712516370
GD_DGBI_Yes	VIP_Lamina_properia	GAP43_muscularis_mucosa	-0.25714286	0.354860364
GD_DGBI_Yes	VIP_Lamina_properia	GAP43_Crypt	-0.15294118	0.571744619
GD_DGBI_Yes	VIP_Lamina_properia	GAP43_Lamina_properia	-0.06176471	0.820241878

Declaration of AI and AI-assisted technologies:

During the preparation of this work, ChatGPT was used (version 5.2) to assist with generating R code and figure preparation, alongside with QuillBot to support proofreading and correction of grammar and spelling. All content produced with these tools was carefully reviewed and edited by me, and I take full responsibility for the final content of this thesis.